Interaction of Clay Wash Load with Gravel Beds

Christian Mooneyham

Thesis submitted to the Faculty of the
Virginia Polytechnic Institute and State University
in partial fulfillment of the requirements for the degree of

Masters of Science
in
Civil Engineering

Kyle B. Strom, Chair
Erich T. Hester
Tess M. Wynn-Thompson

December 6, 2016
Blacksburg, Virginia

Keywords: clay, kaolinite, cohesive sediment, gravel bed, wash load

Interaction of Clay Wash Load with Gravel Beds

Christian Mooneyham

ABSTRACT

This study focuses on the interaction of wash load particles with gravel bed rivers. The effects of excess fine sediment loading to streams on general water quality, contaminant transport, and benthic organism mortality has been well examined. A fundamental assumption in fluvial geomorphology and river engineering is that wash load particles ($d < 63\mu m$) do not deposit to stream beds, but are instead transported downstream until they deposit in reservoirs or estuaries. The goal of this study is to determine if wash load sized particles can deposit to gravel beds, where within the bed substrate deposition occurs, under what hydraulic conditions it occurs, and how the composition of the bed affects the spatial and temporal deposition pattern. Further, this study attempts to quantify the mass flux of wash load to the bed based on a simple mass conservation model using the aforementioned conditions as model parameters. This was accomplished through a series of experiments in which a mixture of pure kaolinite clay was allowed to deposit at constant shear over an acrylic, gravel, or sand-gravel mixture. Discharge was then increased to determine the effects of increased bed shear stress on deposited material and further wash load interaction with the bed.

Results indicate that wash load will deposit to acrylic, gravel, and sand-gravel beds during conditions where no bedload movement is occurring. Bed composition is the primary factor controlling the mass flux of wash load from the water column to the bed. Deposition

on acrylic beds forms clay ripples which translate downstream, while deposition in porous beds occurs primarily within the bed substrate. Shear stress also affects mass flux and the magnitude of its effects are related to the bed composition. Discharge increases below the threshold of bedload movement only cause large scale entrainment of deposited particles over non-porous beds. Periods of higher discharge over porous beds result in continued deposition within the bed substrates.

This research enhances not only our knowledge of sediment processes within fluvial systems, but also allows for the quantification of the wash load portion of those processes given minimal initial condition information. The model developed here may be used within larger hydrologic models when examining contaminant spills or mass loading of stream networks with wash load to estimate the mass deposition to the bed. Instances where wash load is contaminated the mass of contaminated sediment retained by the bed is of great importance to local communities given a reliance of residents on that water source for water, livelihood, and recreation.

Interaction of Clay Wash Load with Gravel Beds

Christian Mooneyham

GENERAL AUDIENCE ABSTRACT

This study investigates what happens when very small clay particles enter a stream. Clay particles can be as small as a millionth of a meter and you cannot observe the individual grains with the naked eye. Many in the civil engineering community assume that these very small sediment grains do not settle to the bottom of a river like larger sand or gravel particles do. Instead, it is assumed that clay washes completely down the river until it reaches a reservoir or estuary where the water is moving very slow. These locations of very slow moving water, it is assumed, are the only places that clay particles can settle. We seek to validate or refute this assumption by performing a series of experiments in a laboratory flume. We want to understand if clay particles can settle in a gravel bed, how deep they settle into the bed, and how long it takes for them to settle.

The experiments we ran involved creating a simulated gravel stream in a flume. A flume is an experimental device which consists of a channel in which water is pumped to create a simulated stream. Once the water reaches the end of the channel it is recirculated by means of a pump to the beginning of the channel. Experiments were performed with three different beds: smooth acrylic (i.e. Plexiglas), gravel, and a sand-gravel mixture. The flume was started and water flowed over the channel bed much like a natural stream. Clay was then added to the water. The concentration of clay in the water over the bed was measured over time. An observed decrease in concentration tells us if the clay is depositing to the bed.

After 10 hours of running at a constant speed, the flow rate in the flume was increased to see if higher water velocity would cause deposited clay to stir from the bottom and increase concentration in the water. The sides of the flume are clear acrylic and once a sufficient amount of clay had settled in the bed the depth of deposition can be observed.

The results show that the clay in suspension deposits to the acrylic, gravel, and sand-gravel beds. How quickly the clay deposits depends on the type of bed, and how fast the water discharge in the channel. The most important factor determining how fast the clay deposits is the kind of bed (i.e. gravel, sand-gravel, etc.). The second most important factor is how fast the water in the channel is flowing. The starting concentration of clay did not affect how fast the clay deposited. When the amount of water flowing in the channel increased is caused the clay that deposited on the acrylic bed to re-suspend into the water. This was not the case for the gravel or sand-gravel beds.

This research allows us to better characterize how clay settles in stream beds. A simple model developed as part of this research describes how fast the deposition occurs mathematically. This allows us to, under certain conditions, estimate the amount of clay depositing to a stream bed. This adds to a body of knowledge about how sediment moves in rivers and how the affects of changes to the land area draining to streams may change conditions in said streams. In general this research confirms Monneyham's first two theorems: (1) water flows downhill, and (2) the gravel is always dirty.

Acknowledgments

I would like to express great appreciation to my advisor Dr. Kyle Strom for his tireless assistance and the innumerable hours he spent helping guide me through the research process. A student could not ask for a more patient, thoughtful, and dedicated advisor. He is a rare person who can find not only the utility in engineering but also the beauty in the earth processes which we study. I would also like to thank my committee members, Dr. Erich Hester and Dr. Tess Thompson. Thank you for your time in guiding my research. I enjoyed working with you and appreciate the different perspectives you brought to my studies.

Additionally, I would like to thank my fellow graduate students with special appreciation to Duc Tran and Nilay Iscen for their help in getting me familiar with the lab and the experimental process, and in engaging in productive discussion with me. I would also like to thank Brandon Dillon who has always been there with much appreciated advice and whose friendship has made my time at Virginia Tech especially memorable.

I would like to thank my parents for their love and encouragement in helping me pursue my dreams. Finally, I would like to thank my wife, without whose tireless love and support I would not have been able to complete my Masters Degree.

Contents

List of Figures

List of Tables

1 Introduction

1.1 Overview

Anthropogenic land use changes within watersheds (e.g., logging, agriculture, and mining) can increase the loading of fine particles such as silt and clay (referred to in this study as fines) to streams and rivers (Platts and Megahan, 1975). This additional loading primarily occurs in pulses during storms or final snow-melt when fine sediment is carried off hill slopes with runoff. The introduction of pulses of fine sediment can also come from the failure of mine tailing ponds, river bank failure, and the decommissioning and removal of dams. In particular, large volumes of silt and clay sediment that get trapped upstream of dams can become mobilized and introduced to the downstream fluvial system upon dam removal. This is true when removing both larger hydroelectric projects such as those in the Pacific Northwest, or the smaller mill-pond type installations that are common on the East Coast of the United States.

The addition of such fines has been shown to have ecological effects on fish species populations and their distributions (Berkman and Rabeni, 1987; Wood and Armitage, 1997). Many fish species such as salmon lay their eggs in gravel patches called redds. These areas must be porous and oxygenated from interactions between surface and groundwater in order for the eggs to survive. Accumulation of fine particles reduces the oxygenation process and

can cause high mortality rates (Westrich and Förstner, 2007). Furthermore, heavy metal contaminants may become attached to cohesive sediments and stored within the river system and require later remediation (Peng et al., 2009; Salomons and Stigliani, 2012). Clay to silt sized particles (sometimes referred to as wash load) have been associated with lead and copper contamination (Merrington and Alloway, 1994). Contaminant movement associated with sediment transport can account for as much as 90% of the total contaminant transport in certain, mining affected, rivers (Trefry and Presley, 1976; Hudson-Edwards, 2003). Movement of contaminants associated with deposition and entrainment from banks, floodplains, and fine sediment accumulation around in-stream wooded debris has caused persistent spreading of contaminants in some rivers even 60 years after industrial contamination ceased (Skalak and Pizzuto, 2010; Pizzuto, 2014). The deposition and resuspension of fines within and along stream beds are thus important processes to understand in the study and maintenance of stream ecosystems.

Understanding the mass flux of fines into gravel beds as well as the retention and re-suspension characteristics of said fines, during various stream flow conditions, will lead to a better understanding of the short and long term ecological effects associated with fine sediments. It will also lead to a better understanding of contaminant distribution within gravel beds and how such contaminants may be retained in low order streams and/or move downstream as wash load.

1.2 Suspensive and Depositional Forces

To understand the movement of particles in the water column one must first understand the forces which cause these particles to suspend and deposit. Turbulent flows can be described as having three dimensional fluctuating velocities within the mean fluid motion. In a standard Reynolds decomposition, the total fluid velocity is taken as the summation of the time average velocity and a fluctuations about this mean:

$$U_i = u_i + u_i' \tag{1.1}$$

where U_i is the total instantaneous fluid velocity, u_i is the time average velocity, and u_i' is the time varying fluctuating component; here i ranges from 1 to 3 in association with the primary orthogonal directions of x, y, and z and the directional velocity components u, v, and w. In simple gravity driven river flow over a plane bed, the primary factor contributing to the maintenance of fine particles in suspension is the upward fluctuation in fluid velocity w'. The magnitude of these fluctuations can be characterized by the root mean square (RMS) of the fluctuations $\sqrt{\overline{w'^2}}$; here, the over-bar notation represents time averaging. The RMS value of w' does not have directionality, but instead represents the intensity of vertical fluctuations. These fluctuations work to mix suspended sediment in the vertical direction. The RMS of the vertical turbulent velocity is typically linked to mean flow quantities through the shear velocity ($u_* = \sqrt{\tau/\rho}$, where τ is the bed shear stress and ρ is the fluid density). The maximum vertical RMS turbulence fluctuations are approximately equal to u_* for smooth

and rough boundary conditions (Antonia and Luxton, 1971). The force which opposes turbulent mixing in the vertical is gravity. The rate at which gravity pulls sediment to the bed in a quiescent body of water is quantified by the particle's terminal settling velocity, w_s. Common convention suggests that when $w_s/u_* \gg 1$, it is likely that the particles will settle out of suspension, and when $w_s/u_* \ll 1$ one can say that vertical mixing dominates over gravitational settling (i.e., the suspension is well mixed). These suspensive and settling characteristics have been quantified with the Rouse Number (P) which takes the ratio of w_s to u_* scaled with the von Karman constant (κ):

$$P = \frac{w_s}{\kappa u_*} \tag{1.2}$$

The Rouse number that is typically taken as the transition point between bed load and suspended load is 2.5. This corresponds to a 1:1 balance between w_s and u_*. Values below this indicate instances where the shear velocity is much higher than the sediment settling velocity. As these values decrease from 2.5 to 0.001 the concentration profile of sediment moves from stratified (with higher concentrations of sediment near the bed and lower concentrations at the surface) to a near uniform distribution of sediment within the water column (Middleton and Southard, 1984). The calculated change in concentration profiles according to the Rouse solution of the advection-diffusion equation for suspended sediment is shown in Figure 1.1.

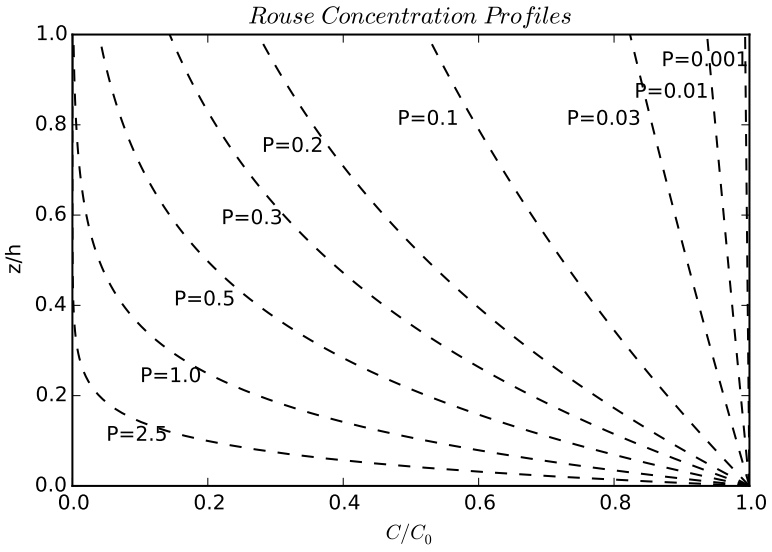

Figure 1.1: A plot of the Rouse suspended sediment concentration profile under equilibrium conditions for a series of Rouse numbers (P).

1.3 Wash Load

An overarching goal of my research is to examine the interaction of so-called "wash load" (as it has been practically defined) with different types of beds. Conceptually, wash load is material that originates from some location other than the bed, and is assumed to wash completely out of the river system without depositing (Einstein et al., 1940). This is differentiated from bed load, which is bed material that moves along the bed by rolling or saltating, and suspended bed-material load, which consists of particles that entrain from the bed and then re-deposit on the bed at some point downstream (Middleton and Southard, 1984). The wash load concept is based on the idea of a balance between sediment supply rate and sediment transport capacity of the flow. One can conceptually consider a continuum of flow transport capacities which are a function of particle size. One can also conceptualize a

similar relationship of sediment supply from the drainage basin as a function of particle size. The location where the sediment supply and carrying capacity curves intersect is a critical sediment size below which the carrying capacity of the flow far exceeds the supply rate (Figure 1.2). Sediment sizes below this critical value will, within this framework, theoretically never deposit on the channel bed (Shen, 1971).

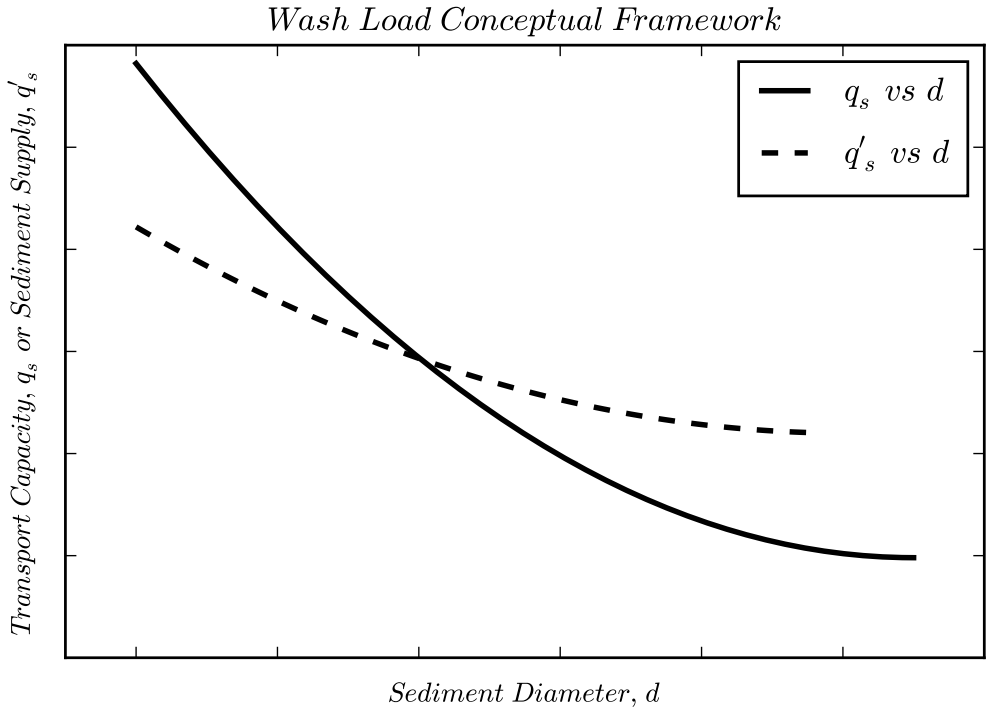

Figure 1.2: Wash Load Conceptual Framework, adapted from Shen (1971).

Determining this critical sediment size based on these factors can be difficult because it is difficult to quantify the sediment supply rate from the basin. Several methods exist to estimate the size of wash load based on the size characteristics of a given river bed. For example, one may define wash load by some small size fraction of the bed material (e.g. d_5). This implies that wash load particles are not found in appreciable quantities in the bed.

That said, wash load is typically associated with those particles finer than 62.5 μm (i.e., silts and clays) (Shen, 1971). This make sense as silt and clay particles are not generally found in appreciable quantities in gravel bed streams (Shaw and Kellerhals, 1982; Carling and Reader, 1982). That said, they can be found in appreciable quantities in gravel bed streams where the watershed has been altered by land use change (Carling and Reader, 1982). For the purposes of this study, "wash load" is practically defined as suspended clay and silt particles.

Working from the definition of wash load as those particles finer than 62.5 μm (noting that wash load particles can be cohesive), engineers assume that wash load does not interact with stream beds (Garcia, 2008). Instead, they assume that wash load only settles on stream banks and on floodplains (Garcia, 2008; Colby, 1957; Lambert and Walling, 1988). This is based on the idea that sand and gravel are more morphologically important than clay and silt, and the very low Rouse numbers that typically exist for sizes less than 62.5 μm. For example, Rouse numbers for wash load under hydraulic conditions similar to those in this study (i.e., in a wide channel with slope $S_0 = 0.0001$ and depth $h = 0.64$ m) are on the order of $P = 10^{-8}$. This indicates that the suspensive characteristics of the flow dominate over the depositional qualities of the individual particles, and that the particles are fully dispersed and well mixed over the entire depth of the water column (Figure 1.1). This enumeration of depositional characteristics of clay and silt combined with the lack of such particles in the bed indicate that the assumption that wash load does not settle in gravel beds is reasonable.

However, there are situations in which this may not hold true. These include instances

where a pulse of suspended sediment of sufficiently high concentration is introduced to the flow such that the carrying capacity of the fluid cannot keep all of the fine particles suspended. Such instances may include controlled dam removals or contaminant loading such as that caused by the EPA in the Animas River, Colorado due to a mine tailing pond failure. Additionally, some research using dilute solutions of suspended clay have indicated that wash load particles can settle and interact with both sand (Packman et al., 2000b,a) and gravel beds (Packman et al., 2004; Krishnappan and Engel, 2006; Krishnappan, 2007). However, (1) little work has been done to examine mechanisms associated with the capture of mud other than exchange between surface and ground water due to heterogeneity in the hydrostatic pressure distribution on the bed; and (2) few have examined methods to quantitatively account for loss of suspended wash load to the bed within sediment transport theory. In this work I focus on understanding and quantifying the transfer of clay wash load from a suspension to a porous bed. In doing so I will experimentally test the settling characteristics of wash load flowing over a gravel bed and model the mass accumulation of suspended sediment in the bed over time.

1.4 Research Questions

The focus of this research centers on movement of clay wash load and its interaction with gravel beds. The overarching question asked by this research is, does clay wash load, traveling in a well mixed suspension, interact with gravel beds? That is, does any of the wash load deposit out within the bed? My primary hypothesis is that suspended clay material can

indeed be sequestered within gravel beds. Overall, the literature discussed in the following section supports this primary hypothesis. Knowing this, the primary research question is further broken down into three separate parts to guide the experimental development and data interpretation. The three sub-questions this study seeks to answer are:

Research Question 1: Is the net loss of suspended clay to the bed a function of shear stress, bed characteristics or initial concentration? **Hypothesis 1:** The loss of suspended clay to the water column is a function of the bed shear stress and the bed characteristics, but the loss of clay to the bed is not a function of initial concentration. **Rational:** The deposition of sediment from the water column to the bed is taken as a balance between depositional and erosional forces acting simultaneously on the suspended material. Higher shear stress, associated with higher RMS vertical fluid fluctuations, will increase the suspensive forces acting on the wash load particles causing a decrease in deposition. The ability of particles to deposit and remain deposited will depend on the characteristics of the bed into which they will settle. Settling on non-porous beds leaves deposited particles exposed to the brunt of the bed shear stress while porous beds may allow particles to settle into interstitial voids and hide from entraining forces. Finally, we can model mass flux to the bed with local concentration and settling velocity alone. In other words, the fractional decay of mass in the water column is not a function of the initial concentration.

Research Question 2: Where in the bed does deposition occur? **Hypothesis 2:** Settling will most likely occur within the substrate if the characteristics of the suspended sediment and void space in the bed allow for static percolation. **Rational:** Suspended

particles can only be expected to settle into the interstitial voids of a bed substrate if the voids are significantly larger than the settling material. If this is not the case or the bed is non-porous the settling particles will clog the bed and collect on the surface.

Research Question 3: Can deposited fine material be entrained with increases in bed shear stress? **Hypothesis 3:** Once suspended wash load has deposited in a porous bed it cannot be re-entrained while the bed surface material is immobile (i.e., no bedload movement occurs). That said, deposition on surface grains or on non-porous beds will be available for entrainment. **Rational:** Hiding effects prevent the entrainment of wash load deposited in interstitial voids. If the bed layer moves and the gravel particles on which the wash load deposited begin to move it is likely that the deposited sediment, now exposed to the turbulent effects of the flow and the agitation caused by moving grains, will entrain to the water column.

I examined these questions by conducting a series of laboratory experiments in a re-circulating flume. To do so, a solution of kaolinite clay was introduced to the flume system to mimic wash load flowing over a set of different bed types. The change in the clay concentration was observed over a period of constant bed shear stress followed by a series of periods of increased bed shear stress. Observed concentration and suspended sediment sizes changes over various hydraulic conditions allowed me to flesh out the aforementioned hypothesized relationships. Before discussing the experimental methodology, I first present some additional background information pertinent to the transport of fine clay particles and the movement of finer sediment within a coarser gravel framework.

2 Background

Further background from the literature is given below regarding what is known about (1) the deposition of clay on solid and porous beds; and (2) the location of sand deposits that infiltrate gravel beds. The first item is included to show fundamental concepts as well as experimental and field work performed by others to characterize the settling of clay in estuarine and marine settings. Most of this work took place in experimental annular flumes that had solid, non-porous beds. This summary focuses on the work by Krishnappan, Lau, Mehta, Partheniades, and Packman. The second item examines physical factors which must be considered when thinking about where clay might settle to in a gravel bed.

2.1 Clay Settling Characteristics

Much research has been done to experimentally examine the deposition (Mehta and Partheniades, 1975; Lau and Krishnappan, 1992, 1994; Haralampides et al., 2003; Garcia-Aragon et al., 2011) and entrainment (Krishnappan, 2000; Lau and Krishnappan, 1994) of cohesive, clay sediment. Most of these experiments were conducted in rotating, annual flumes with smooth nonporous beds. A key element of these studies was the examination of clay floc formation within in the water column and the impact of such flocs on deposition. As such,

the context for this body of work has been that of estuarine, coastal, and marine settings. Early work done by Mehta and Partheniades (1975) and Lau and Krishnappan (1992) indicated that settling of flocs caused suspended concentration of clay to decay exponentially to an equilibrium concentration. Other work has shown that for certain bed shear stresses the suspended sediment concentration can decay to zero (Lau and Krishnappan, 1994; Krishnappan, 2000) or may decay to zero if given sufficient experimental run time (Garcia-Aragon et al., 2011). The concentration decay approaches a final equilibrium (either zero or non-zero) which is a function of the type of suspended sediment, the bed shear stress, and the initial concentration (Lau and Krishnappan, 1992; Mehta and Partheniades, 1975). Schools of thought describing the settling of clay particles generally falls into one of two schools of thought based on the interaction of settling and suspensive forces: simultaneous or mutually exclusive deposition and entrainment. The former asserts that cohesive, like non-cohesive, sediments can be depositing and eroding from the bed at the same time; the latter asserts that erosion and deposition do not occur at the same time.

2.1.1 Mutually Exclusive Deposition and Entrainment

The theory for mutually exclusive deposition is originally based on a series of experiments conducted by Partheniades (1965) and Partheniades et al. (1968). In these experiments, clay was suspended in a rotating flume and allowed to deposit at a certain shear stress. When the concentration in the flume reached an equilibrium, the water sediment mixture was exchanged with clear water. This clear water was then observed to remain clear for the duration

of the experiment. Likewise, deposited clay was entrained to a point of equilibrium and the water was exchanged for clear water and remained clear. These results indicated that once decay had reached equilibrium, no further entrainment occurred. Likewise, once entrainment reached equilibrium, due to increased shear stress, no further deposition occurred.

Lau and Krishnappan (1992, 1994) showed in flume experiments that deposition over time caused a reduction in the size of the particles within the water column with time. They interpreted this as an indication that as flocs form and settle they are not broken apart and re-entrained. They further observed that larger flocs tended to settle out more readily than smaller flocs, causing a reduction in the d_{50} value over time. Similar results were also later found by the same group in the study of Haralampides et al. (2003), where it was observed that size of the material in suspension tended to fine with time. They reasoned that this fining of particle sizes in the water column supported the hypothesis of mutually exclusive deposition and resuspension. If entrainment were occurring simultaneously with deposition the larger particles or flocs would be broken apart into smaller pieces and re-entrained over the coarse of the experiment. This would cause the smaller size fractions to either remain the same or increase in number, as opposed to decreasing. One can infer from these experiments that entrainment of particles was not occurring simultaneously with deposition (Lau and Krishnappan, 1994).

Krishnappan (2000) experimentally determined the minimum bed shear stress, below which all of the sediment will settle out, for naturally occurring fines in the Athabasca River. The conclusion being that at and below a certain critical shear stress of deposition

the re-entrainment characteristics of the flow are so minimal that complete removal of the suspended wash load will occur. For shear stresses below this value the exponential decay of suspended sediment in the water column reaches zero. Likewise any increase in shear stress above a critical shear stress of erosion will cause the entrainment of deposited particles. These experiments are limited to flume tests with an impenetrable Plexiglas bed. These simulations of sediment interaction are limited in that they do not consider increased bed shear due to the roughness layer or deposition within a bed substrate. Later experiments with gravel (8mm) and sand (1mm) beds showed that both beds had relatively high rates of entrapment of Kaolinite wash load (Krishnappan and Engel, 2006; Krishnappan, 2007).

The concentration decay of sediment in the water column (and inversely the accumulation of mass in the bed) has been described as a function of the sediment settling velocity (w_s), concentration in the water column (C), flow depth (h), and the bed shear stress (τ_b). Bed shear stress has specifically been important given its value relative to critical shear stresses of deposition (τ_d) and entrainment (τ_e) as described above. That is, for the case where $\tau_b < \tau_d$ the water column concentration will decay to zero. For cases where $\tau_d < \tau_b < \tau_e$ the water column concentration will reach some point of equilibrium. Finally, for cases where $\tau_b > \tau_e$ there will be erosion. Krishnappan (2000) notes that for natural sediments in the Athabasca River $2 * \tau_d \approx \tau_e$ and at approximately $6\tau_d$ no sediment will deposit on the flume bed. This conclusion is described by a mass conservation modeled in Equation 2.1:

$$\frac{\partial \overline{C}}{\partial t} + \frac{\partial F_i}{\partial x_i} = 0 \tag{2.1}$$

Where $F_i = (\overline{u_i} + w_s\delta_{i3})\overline{C} + \overline{u_i'C'}$ represents a flux vector averaged over turbulent timescales. The first term of this flux vector considers average velocities accompanied in the vertical direction by settling velocity of the sediment particles (w_s) and is advective in nature. The second term represents the Reynolds fluxes and is diffusive in nature. The latter term is modeled as being linearly proportional to the concentration gradient in the water column. That is, $\overline{u_i'C'} = -D_d\frac{\partial\overline{C}}{\partial x_i}$, where D_d is the kinematic eddy diffusivity. Given these methods of particle movement one can model the boundary condition at the bed as the balance between depositional and erosive forces (Eqn 2.2).

$$F_{sz}\,|_{z=b} = E_r - D_r \tag{2.2}$$

$$D_r = w_s C_b \tag{2.3}$$

$$E_r = \overline{w'C'} = D_d\frac{\partial\overline{C}}{\partial x_i} \tag{2.4}$$

This was applied to cohesive particles by Krone (1962) with a depositional model using the critical shear stress of deposition discussed above.

$$\frac{\partial h\overline{C}}{\partial t} = -D = w_s C_b\Big(1 - \frac{\tau_b}{\tau_d}\Big) \tag{2.5}$$

2.1.2 Simultaneous Deposition and Entrainment

The theory for simultaneous deposition and entrainment of cohesive sediment is originally based on experiments by Krone (1962). In these tests it was shown that the fraction of

suspended sediment deposited over time decreases with increased bed shear. The cause of this was concluded to be a balance between depositional and erosive forces occurring simultaneously. As bed shear stress increased the erosive forces increased and offset the depositional forces. Later Krone (1993) would conduct tests marked with a radioactive gold tracer. A concentration of sediment was suspended and allowed to settle at a constant shear. Tracer particles were then added to the flume. The tracer particles decreased in concentration at a higher rate than the total concentration of particles. During this time erosion of previously deposited untraced particles caused the overall deposition to occur slower than the tracer particles added later in the experiment.

The case for simultaneous deposition and erosion is confirmed by field studies conducted by Sanford and Halka (1993). They showed that in field conditions suspended sediment concentrations began to decay as soon as bed shear stress began to reduce from a peak value. This means that deposition was occurring at values greater than the critical shear stress for entrainment. If erosion is mutually exclusive from deposition then no deposition should occur if the shear stress is in a range for which only erosion should occur. This is seen mathematically in Equation 2.5. When shear stress reaches the critical bed shear stress the depositional term goes to zero. Modeling shear stresses above this with the depositional model results in only increasing concentration values. Based on this evidence Winterwerp and Van Kesteren (2004) reject the idea of mutually exclusive flux properties of cohesive sediment. They contend that clay interaction with the bed is based on simultaneous deposition and erosion where deposition is continuous and entrainment is based on bed shear stress exceeding

a critical value.

2.1.3 Filtering Models

A third school of thought may be said to exist outside of the deposition-entrainment debate which characterizes interaction of suspended sediment particles and a bed by means of surface-groundwater exchange (Packman and Brooks, 1995; Packman et al., 1997, 2000b,a). Hyporheic flow, caused primarily by heterogeneity in the pressure at the bed surface due to such obstructions as bedforms and large woody debris, has been shown to occur in very porous beds in the absence of bedforms (Nagaoka and Ohgaki, 1990). Elliot and Brooks (1997) model the advective flow of surface water into the hyporheic zone as as driven by a sinusoidal pressure distribution over a flat bed. Packman and Brooks (1995) show qualitatively that sand beds in the presence of bedforms can filter suspended clay particles from surface water as a result of advective pumping, or hyporheic flow (Packman and Brooks, 1995; Packman et al., 1997). Packman et al. (2000b) uses Elliot and Brooks (1997) as a basis to develop a colloid exchange model which treats the clay exchange with a bed as a filtering process and predicts the rate of exchanged based on the morphodynamic characteristics of the bed forms. Packman et al. (2004) showed that solute exchange with flat gravel beds was consistent with both diffusive and advective characteristics. Qualitative dye experiments showed evidence of advective flowpaths in a flat, unarmored gravel bed due to some unseen bed irregularities. The results were fit to the hyporheic exchange model but only worked for bedform wavelengths which did not exist physically in the experiments.

The idea of an armor layer created by coarsening of surface grains in gravel bed rivers has been well explored in the literature. The work of Church and Hassan (1998) showed that bed load of coarse armor grains re-ordered the armor layer into a stable arrangement of stone cells that accounted for approximately 15-25% of the stream bed composition. In flume experiments with uniform bed composition Dermisis and Papanicolaou (2014) showed the presence of such irregularities in surface layer stone arrangement and size could lead to localized sand deposition which clogged the surface layer and even pushed sand deeper within the bed. This suggests that an armored layer may be thought of as a bedform in and of itself and that self-stabilizing stone cells within that bedform constitute a series of additional obstructions further enhancing Hyporheic flow and deep deposition of fine particles.

2.2 Deposition, Clogging, and Entrainment of Sand and Silts in Gravel Bed Rivers

Several studies have been conducted to examine the clogging of gravel beds by sand and fines which create a barrier to continued infiltration of subsequent fines (Lisle, 1989; Barzilai et al., 2013). In Barzilai et al. (2013), field investigations showed clogging of the surface layer in intermittent streams during reduced precipitation rain seasons. These fines were later re-mobilized during high flow storm events, returning the bed to apparently normal conditions. Likewise, research performed by Lisle (1989) showed instances where the top layer of gravel beds were clogged with sand and silt. Much of this material does not move completely downstream in one continuous process but moves as a series of entrainment and

deposition cycles along the river reach from low to higher order streams. Post hydrograph return to base flow conditions causes much of the suspended and wash load to settle on the bed surface where it can be remobilized during subsequent hydrological cycles (Lambert and Walling, 1988). However, the research done by Lambert and Walling (1988) only considered the top 10 cm of the bed surface. Work by Beschta and Jackson (1979) showed that much of the fine material deposited during low flow periods was removed after peak flow events. This supports the surface deposition and periodic movement of fines investigated by Lambert and Walling (1988).

Other flume and field studies, however, have shown that very fine particles can settle through the pore space voids well below the bed surface (Lisle, 1989; Carling and Reader, 1982; Einstein, 1968). Lisles research showed many instances where fines less than 2 mm (i.e., fine sand and silt) could infiltrate up to 25 cm deep into naturally occurring stream bed substrates. Such infiltration occurred during small storm events where sediments large enough to clog the interstices of the substrate were not suspended (Lisle, 1989). These differing field and experimental results seem to indicate that interactions of wash load particles not only move much of the fine material out of lower orders streams but also allow for some fine interaction with the gravel bed and deposition into the bed substrate.

When considering the interaction of the bed one must understand the characteristics of gravel beds and how these characteristics can affect mass flux at the sediment-water interface. One would expect that the vertical, spatial deposition of suspended sediment within the bed would be based on the characteristics of the suspended grain in relation to that of the bed

material. One would not expect a suspended particle to settle within the voids of a bed if that particle were the same size or larger than the void space created by the bed particles. To that end an examination of bed material and suspended material is required.

Gravel beds can be described as unimodal or bimodal. The former means there is only one characteristic size of sediment compositing the bed (i.e., gravel sized particles); the latter means there are two characteristic grain sizes which make up the bed (i.e., appreciable quantities of both sand and gravel) (Parker and Andrews, 1985; Parker, 2008). The modes of the latter do not necessarily exist in a well-mixed state along the bed depth. The surface grains are usually much larger and form an armor layer. Below the armor layer are the finer, sand size particles which are mixed amongst a framework of larger gravel particles. This is caused by selective fining of the surface during bed load transport where finer grains are more frequently transported than the coarser grains (Tait et al., 1992; Leopold, 1992). Smith et al. (1997) defined the degree of bimodality of a stream bed based a relationship between the size fraction of the modes and the proportion of the total bed included within that mode as

$$B^* = \mid \phi_2 - \phi_1 \mid (F_2/F_1) \tag{2.6}$$

Where ϕ_1 and ϕ_2 represent the four largest, continuous 0.25ϕ bins comprising the primary and secondary modes of the bed, respectively. The terms F_1 and F_2 represent the fractional proportions within the primary and secondary modes, respectively. In defining the subscripts this way the critical bimodality term B^* self-correct for fine and coarse dominated bimodal beds while keeping the same range of critical values to define bimodality ($B^* = 1.5 - 2.0$).

In this research a unimodal and quasi-bimodal bed types will be examined. The gravel bed test only has a single mode in the gravel size range and as such the relationship in Equation 2.6 is not applicable. The sand-gravel mixture has two modes (one in gravel size range and one in the sand size range). The bimodality measure for this mixture is $B^* = 0.41$.

Much research has been done to examine the relationship between sediment characteristics of the bed and suspended sediments to determine whether the fine sediment will deposit unimpeded within the bed substrate or form a surface seal (Gibson et al., 2009; Huston and Fox, 2015). Gibson et al. (2009) develops a critical ratio between the d_{85} of suspended sand and the d_{15} of a gravel bed material. The critical values at which depositing sediment begins to form a surface seal are $d_{15,gravel}/d_{85,sand} = 10.6 - 15.4$. Conceptually this associates the finer grains of the sediment bed with the pore space size through which the depositing suspended material must settle unimpeded. It makes sense that the larger characteristic size of the settling material through the space formed by the smaller characteristic size of the bed will govern this settling.

Huston and Fox (2015) also showed that the depth of the fine sediment deposition can be estimated by a bed material diameter to suspended grain diameter ratio. Their research showed that the primary driver of sediment deposition depth was the porosity of the substrate, followed by Reynolds number. By calculating the pore water diameter and comparing to the diameter of fines in suspension they effectively predict when clogging will occur. One of the ratios describing unimpeded static percolation is described below for

hydraulically rough turbulent flow (Equation 2.7)

$$\frac{d_{ss}}{d_{fs}\sigma_{ss}} > 27 \tag{2.7}$$

where d_{ss} is the diameter of the substrate sediment, d_{fs} is the diameter of the fine sediment, and σ_{ss} is the standard deviation of the substrate sediment. This can also be written in terms of the pore water space (Equation 2.8)

$$\frac{d_o}{d_{fs}} > 5.5 \tag{2.8}$$

where d_0 is the pore water diameter. These diamter ratios will be examined later in the experimental methods. For calculation purposes $d_{fs} = d_{fs,85}$, $d_{ss} = d_{ss,15}$, and $\sigma_{ss} = \sqrt{\frac{d_{ss}^{85}}{d_{ss}^{15}}}$.

The literature indicates that wash load particles can, under certain circumstances, deposit within beds of various types. A majority of this work centered on deposition to smooth impervious beds. That said, the depositional characteristics of wash load are still up for debate. Furthermore, little work has been done to experimentally examine the location of deposition spatially within the bed or the effects of different hydraulic conditions and gravel bed types on deposition. Little work has also been done to examine how such particles may entrain from a porous bed.

3 Methods

3.1 Experimental Methods

3.1.1 Overview

The research questions were tested by conducting a series of wash load experiments in a tilting, recirculating flume in the Baker Environmental Hydraulics Laboratory at Virginia Tech. Several different types of data were required to characterize the interaction of the suspended clay with the bed. These include parameters which quantify the concentration in the water column, the suspended and bed sediment size distributions, and the hydraulic characteristics of the flow. By measuring concentration over time for tests with different initial suspended sediment concentrations as well, as differing bed and hydraulic conditions, one can draw conclusions with regard to the impact they have on suspended sediment flux to the bed. Subjecting deposited material to different increasing shear stresses then allows one to determine the impact of increased discharge on deposited material.

The flume used in the experiments consists of a main channel measuring 46 cm wide, 46 cm tall, and 6.1 m long, a downstream water tank, and a recirculating pump controlled by a variable frequency drive (VFD) control system. The flume system tilts on a point of rotation under the downstream tank and is controlled by adjusting two jack screws on the upstream end of the flume. The experimental setup is similar to the flat gravel bed tests

of Packman et al. (2004) and sediment settling tests of Einstein (1968). To introduce clay to the system the flume was started and a suspension of processed kaolinite was added to the downstream tank over one cycle time of the system volume. This was done in order to achieve a well-mixed state in the flume system. Salt tracer tests indicated that after the time period required to achieve a well mixed state there was very slow exchange between the porous beds and the water column which lasted no longer than 60 minutes. Thus observed changes in the suspended sediment concentration during the entirety of the test were not a result of water exchange across the sediment-water interface.

Each test consisted of two phases: deposition and entrainment. The depositional phase lasted approximately 10 hours. During this phase sediment laden water was allowed to flow over a given bed type at a constant shear velocity. The entrainment phase began immediately after the deposition phase with no interruption in flow or data collection. The entrainment phase involved a series of step increases of flume discharge. This increased the water column depth and the shear velocity. Uninterrupted measurement of the aforementioned parameters continued through the entrainment phase. The shear stress was never sufficiently high to cause movement of the bed material.

Parameters which required measurement during these tests included the concentration of suspended sediment in the water column over time, size of the suspended sediments, flow depth, and bed shear stress. Concentration time series data was the primary parameter which allowed the characterization of mass loss in the water column, and conversely the amount of mass gain in the bed. The test conditions varied among (a) three different initial

concentrations, (b) four bed shear stresses, and (c) three bed types. A total of 33 tests were conducted: 12 tests over two different porous beds and 9 tests over the smooth, non-porous, acrylic glass channel bottom. The test parameters used are given in Table 3.1.

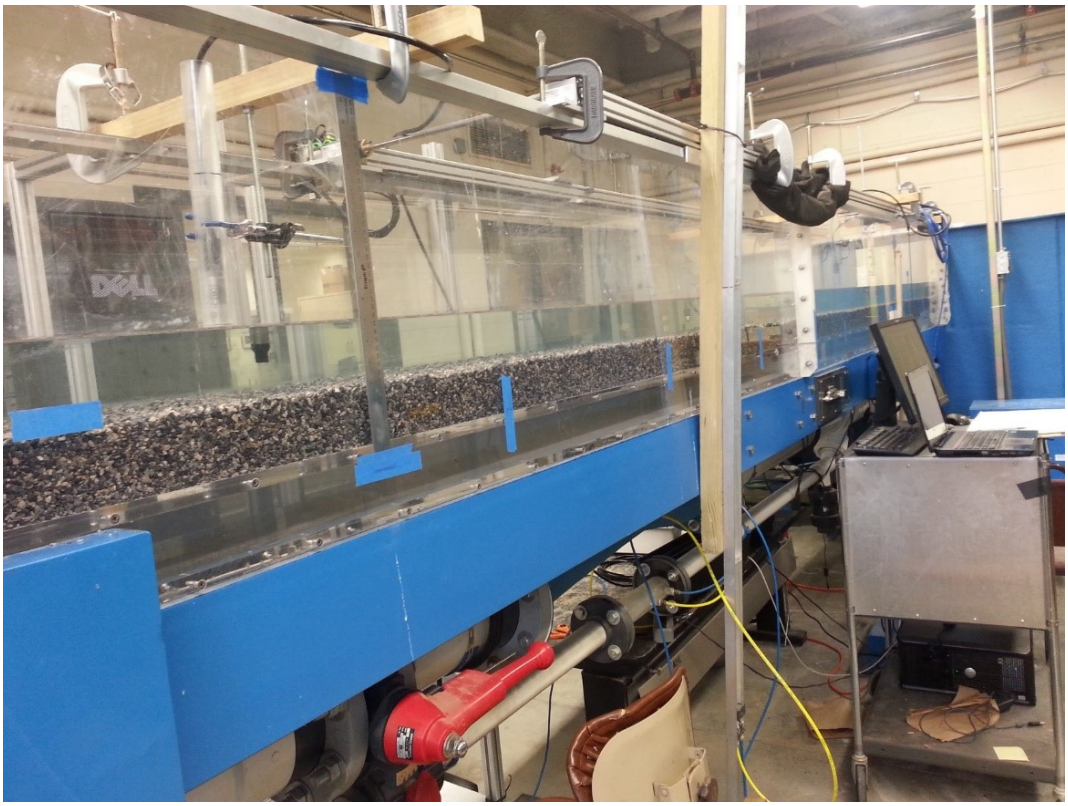

Figure 3.1: Flume channel with unimodal gravel bed. Upstream OBS visible on left.

3.1.2 Flow Characteristics

Flow characteristics were quantified by measuring channel slope, water column depth, system discharge, channel velocity, and shear velocity. Before any of the suspended sediment runs, a series of flume tests were run to characterize the hydraulics of the system at a given bed slope, bed type, and discharge. Hydraulic characteristics were quantified in the following ways. Slope was measured by taking an elevation profile of the flume bed using a Bosch

Test	Deposition						Entrainment			
	u_* (m/s)		C_0 (mg/L)		h (cm)	Q (m^3/s)	u_* (m/s)			
A:LS:LC	0.011	low	101	low	4.64	0.0036	0.013	0.015	0.017	0.018
A:MS:LC	0.015	med	84	low	6.83	0.0092	0.015	nma	0.018	–
A:HS:LC	0.017	high	84	low	9.05	0.014	nma	–	–	–
A:LS:MC	0.011	low	191	med	4.72	0.0038	0.013	0.015	0.017	0.018
A:MS:MC	0.015	med	195	med	6.83	0.0086	0.017	0.018	0.021	–
A:HS:MC	0.018	high	177	med	9.05	0.014	0.019	–	–	–
A:LS:HC	0.011	low	397	high	4.72	0.0038	0.013	0.015	0.017	0.018
A:MS:HC	0.015	med	378	high	6.79	0.0070	0.017	0.018	–	–
A:HS:HC	0.018	high	403	high	8.49	0.012	0.019	–	–	–
G:LS:LC	0.019	low	93	low	3.89	0.0024	0.0207	0.0220	0.0234	0.0240
G:MS:LC	0.022	med	87	low	5.91	0.0077	0.0235	0.0242	0.0263	–
G:HS:LC	0.024	high	88	low	7.30	0.011	0.0263	–	–	–
G:LS:MC	0.019	low	199	med	3.89	0.0024	0.0207	0.0222	0.0236	0.0243
G:MS:MC	0.022	med	192	med	5.91	0.0077	0.0234	0.0242	–	–
G:HS:MC	0.024	high	176	med	7.30	0.011	0.0251	–	–	–
G:LS:HC	0.019	low	411	high	3.81	0.0022	0.0207	0.0221	0.0234	0.0242
G:HS:HC	0.024	high	396	high	7.18	0.011	0.0250	–	–	–
G:MS:HC*	0.021	med	393	high	5.04	0.0055	0.0217	–	–	–
G:VHS:LC	0.033	very high	88	low	9.13	0.0162	–	–	–	–
G:VHS:MC	0.033	very high	192	med	9.13	0.0162	–	–	–	–
G:VHS:HC	0.033	very high	363	high	9.13	0.0162	–	–	–	–
SG:HS:LC	0.024	high	93	low	6.99	0.0083	0.0308	–	–	–
SG:LS:LC	0.019	low	87	low	4.41	0.0025	0.0251	0.0265	0.0278	0.0284
SG:MS:LC	0.022	med	88	low	5.95	0.0057	0.0279	0.0286	0.0307	–
SG:LS:MC	0.019	low	199	med	4.45	0.0017	0.0251	0.0266	0.0280	0.0287
SG:MS:MC	0.022	med	192	med	5.95	0.0049	0.0278	0.0287	0.0307	–
SG:HS:MC	0.024	high	176	med	6.99	0.0075	0.0308	–	–	–
SG:LS:HC	0.019	low	411	high	4.41	0.0028	0.0252	0.0266	0.0278	0.0287
SG:MS:HC	0.022	med	396	high	5.95	0.0049	0.0278	0.0287	0.0307	–
SG:HS:HC	0.024	high	393	high	6.99	0.0075	0.0308	–	–	–
SG:VHS:LC	0.028	very high	88	low	9.13	0.0119	–	–	–	–
SG:VHS:MC	0.028	very high	192	med	9.13	0.0119	–	–	–	–
SG:VHS:HC	0.028	very high	363	high	9.13	0.0119	–	–	–	–

Table 3.1: Test parameters for each of the bed tests

Test Naming Convention: Bed Type: Shear: Concentration.
Bed Types: A - Acrylic Bed, G - Gravel Bed, SG - Sand-Gravel Bed. Shear Types: LS - Low Shear, MS - Medium Shear, HS - High Shear, VHS - Very High Shear. Concentration: LC - Low Concentration, MC - Medium Concentration, HC - High Concentration.
nma - no measurement available for given entrainment phase. Dashed lines represent no further entrainment phases. * - Armor layer present

Professional GPL3 self-leveling laser and measuring the downstream length with a tape measure. The slope was measured as overall elevation loss across the length of the flume channel. Slope was later confirmed by comparing the regressed u_* values calculated using measured velocity profiles fit to the log-laws with the slope-depth relationship, $u_* = \sqrt{gRS_0}$, where g is the acceleration due to gravity, R is the hydraulic radius, and S_0 is the bed slope. Water column depth was measured in two locations: one at the upstream end of the channel and the other at the downstream end of the channel. Measurements were taken using two identical rulers affixed to the clear, acrylic glass walls of the flume. Said rulers were marked to an accuracy of 0.8 mm (1/32 of an inch); depth readings were taken at the bottom of the meniscus. The two measurements of depth were used to confirm uniform flow within the channel. During most experiments there was no difference between the upstream and downstream water column depths. At no time did the difference in the measured water column depths exceed 0.4 mm. This maximum allowable change in water column depth is 0.94% and 0.43% of the total water column depth at the lowest and highest flow conditions, respectively. These were both deemed acceptable tolerances to maintain the condition of uniform flow.

Shear velocity was extracted from the velocity profile which was measured with an Acoustic Doppler Velicometer (ADV). Velocity profiles were used to calculate shear velocity (u_*) by fitting measured data to the log-law for smooth,

$$\frac{u}{u_*} = \frac{1}{\kappa} \ln\left(\frac{z u_*}{\nu}\right) + 5.5 \tag{3.1}$$

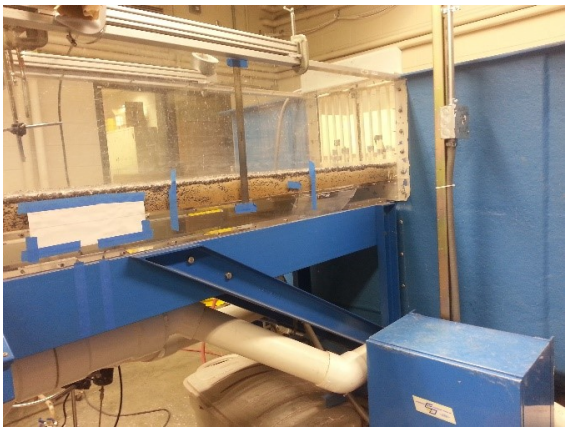

(a) Downstream end of the flume and tank. Sand-Gravel Bed is present in the flume channel.

(b) Pump section from flume tank and recirculation piping

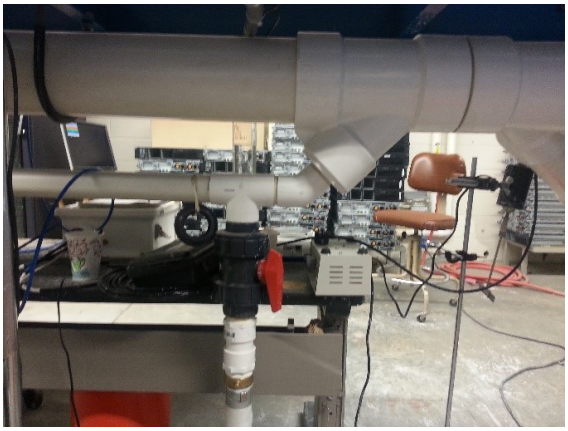

(c) Water distribution pipe splitting to large and small venturi sections and drain.

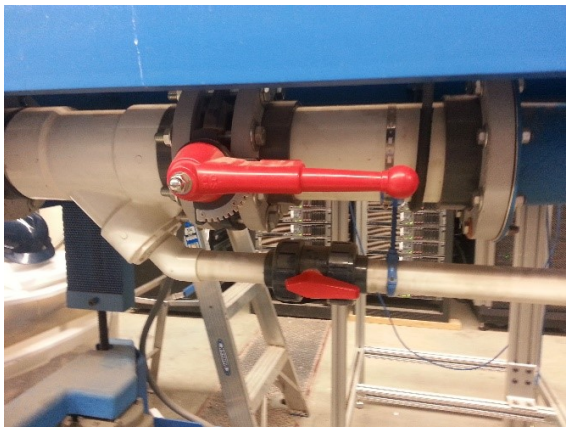

(d) Large and small venturi distribution pipe rejoining prior to the head box

Figure 3.2: Flume Recirculation Path

and rough walls,

$$\frac{u}{u_*} = \frac{1}{\kappa} \ln\left(\frac{z + z_0}{k_s}\right) + 8.5 \tag{3.2}$$

where z_0 is the roughness elevation, k_s is the roughness length scale, and κ is the von Karman constant. The measured average velocity profiles were used to regress the value for u_* as well as k_s. Values of k_s remained relatively constant throughout all regressions and can generally be taken to be approximately $k_s = 2d_{90}$.

ADV readings in the suspension of kaolinite flow over rough porous beds were not optimal. Velocity tests conducted during initial rough bed conditions ranged in average signal to noise ratio (SNR) from 10 to 17 and in correlation (COR) from 50 to 90. Quality data from ADV type instruments has been defined in the literature as having SNR readings above 15 (SonTek, 2001). Data quality varied spatially with depth in the water column, discharge, and clay concentration. That is, data closest to the bed was generally poor and improved as the instrument approached the free surface. Data quality was overall poorest during low channel velocity conditions and improved as channel velocity increased. Finally, data quality was poorest when the concentration was lowest (i.e., at the end of the test when the concentration in the water column had decayed the most) and best when concentration was relatively high (i.e., at the beginning of the test when concentration was near its peak). This final observation is logical as the ADV operates by measuring acoustic backscatter of particles in the water column. The greater the number of particles (i.e., reflectors) the more usable information the ADV has to process and the greater the data quality.

Unexpectedly, the kaolinite provided inadequate backscatter to gather quality data throughout the water column in conditions with the porous bed. In such cases, an attempt to filter the data based on SNR and COR values greater than 19 and 90, respectively, still did not yield satisfactory results. To solve the problem, neutrally buoyant hollow glass spheres (Potters Industries Spherical 110P8) had to be added to the flow as seed material. This was done even in the cases when suspended kaolinite was present. Doing so resulted in SNR values above 19, COR values above 90, and repeatable mean and turbulent statistics

in flows over the rough porous bed. These tests were filtered for SNR and correlation values of 20 and 95, respectively. Each of these tests gave coherent log-shaped velocity profiles and clearly defined log and wake zone regions. These results gave consistent measurements of u_* across the range of channel velocities used in the experiments. This data was then used in a linear regression which related measured depth in the water column to u_*. This process was done separately for both the gravel and sand-gravel bed cases. The acrylic glass bed cases provided adequate in-test data that allowed for acceptable calculations of u_*.

3.1.3 Bed Composition

Three bed types were examined: acrylic glass, open-framework gravel, and a framework-matrix, sand-gravel mixture. The acrylic glass bed case was run as a control test at each discharge. These tests also provided us an opportunity to compare our experimental setup to similar experiments performed by others (e.g., Lau and Krishnappan, 1992).

The gravel used all experiments is an angular crushed stone with a d_{50} = 4.2 mm, d_{85} = 5.5 mm, d_{90} = 5.8 mm and a porosity of 0.41. The sand-gravel mixture used the same gravel but mixed with a coarse sand. The sand-gravel mixture has grain size statistics: d_{50} = 3.3 mm, d_{85} = 4.5 mm, d_{90} = 4.7 mm, and porosity of 0.30. The gravel and sand-gravel beds can be described as unimodal and quasi-bimodal, respectively. This can be seen along with the sieve analyses in Figure 3.3. The sand-gravel bed matches the percent finer by weight pattern as described by Shaw and Kellerhals (1982) for typical gravel beds.

The bed characteristics are quantified in Table 3.2. This table includes threshold values

Bed Type	HF^1	GB^2	$d_{15,bed}$ (mm)	$d_{85,bed}$ (mm)	$\sigma_{ss,bed}$	$d_{85,clay}$ (mm)
Gravel	135	162	3.31	4.74	1.2	0.0205
Sand-Gravel	10.2	28.3	0.58	4.48	2.78	0.0205
Clogging Condition	< 25	< 15.4	–	–	–	–

Table 3.2: Bed Characteristics. [1]The clogging parameter and critical condition based on Huston and Fox (2015), [2]The clogging parameter and critical condition based on Gibson et al. (2009).

which indicate whether suspended kaolinite clay will settle unimpeded through the interstitial voids of the beds as defined by Huston and Fox (2015); Gibson et al. (2009). The results for the gravel and sand-gravel beds differ greatly. For the Huston and Fox (2015) criteria the gravel bed indicates a state of unimpeded static percolation while the sand-gravel test indicates that a surface clogging layer will form. Likewise the Gibson et al. (2009) criteria shows the gravel bed well within the range of unimpeded settling while the sand-gravel bed is slightly above the settling threshold. This indicates that there may be some settling within the sand-gravel bed.

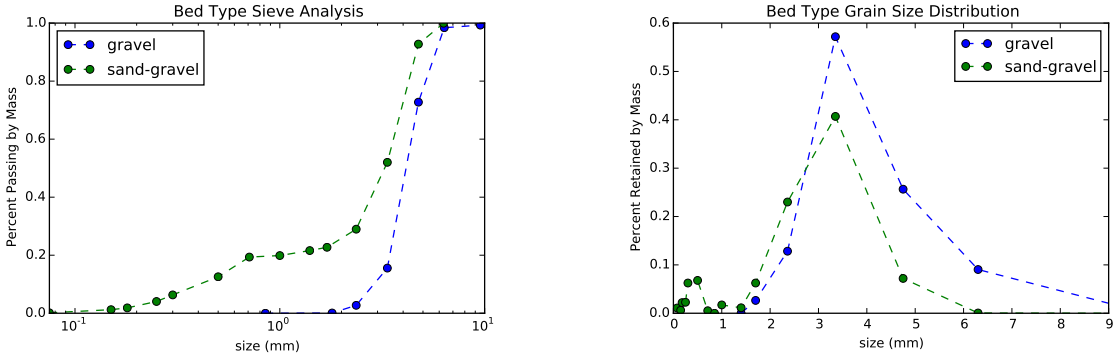

(a) Bed type percent passing by mass, cumulative density function (CDF)

(b) Bed type percent retained, probability density function (PDF)

Figure 3.3: Gravel Bed Size Characteristics

Once placed in the flume the gravel bed remained immobile for all flow conditions. For

the sand-gravel case, water was initially run over the bed for several hours to clear out the sand in the surface layer. This caused an armor layer to form which varied in thickness from one to four times the d_{50} of the surface layer. The armor layer was comprised of the angular gravel particles. A comparison of the bed types can be found in Figure 3.4. Visually one can say that the armor, or surface, layer of the sand-gravel bed has the same characteristics as that of the pure open framework gravel bed. The interface between the gravel armor layer and the sand-gravel mixture substrate will be called the sand layer.

(a) Surface of gravel bed

(b) Substrate of gravel bed

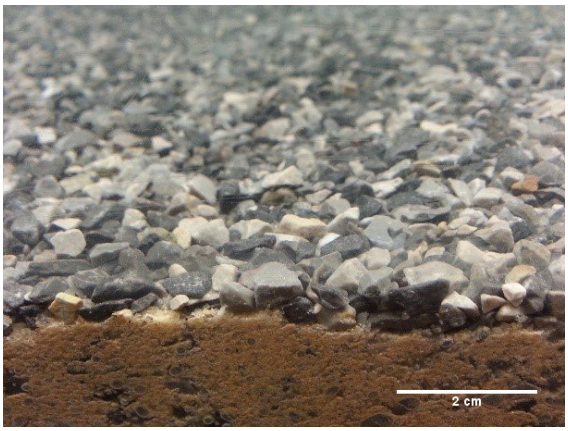

(c) Surface of sand-gravel bed

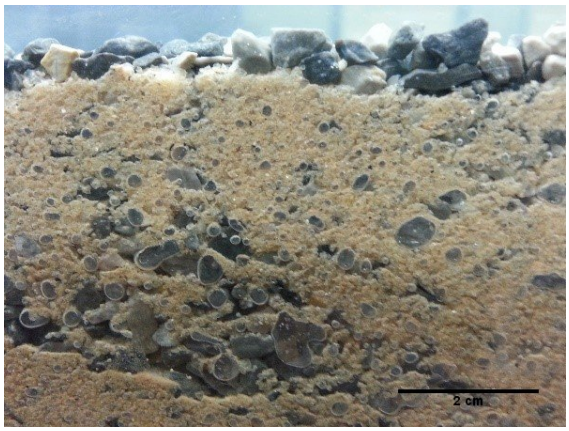

(d) Substrate of sand-gravel bed

Figure 3.4: Gravel and sand-gravel bed types near the surface. Scale is approximate.

3.1.4 Cleaning The Bed

The bed was cleaned after each test to remove deposited clay from the previous test. The acrylic bed was cleaned with a large squeegee between each test to ensure that there was no deposited clay on the flume bed prior to the start of the subsequent test. The flume walls were also cleaned to ensure that no residual clay entered the next test run. Additional tests were not run unless the water in the flume measured within 1 NTU of background conditions for clear water.

The gravel bed was cleaned by running clean water through the flume and disturbing the bed particles through the entire substrate depth. This caused clay in the bed to suspend into the water column and to be carried through the rest of the flume system. The gravel particles were large enough that disturbing them did not cause them to entrain and move out of the flume channel. The clay filled water was drained and replaced with clean water. This process was repeated until no clay entrained from the bed. This method allowed for cleaning of the bed material while maintaining consistent characteristics in the bed substrate.

The sand-gravel bed was cleaned in a slightly different way because of the presence of sand. Disturbing the entire bed substrate of this bed type would cause much of the sand to suspend and move into other portions of the flume system. This would have caused a change in the bed properties over the coarse of the tests. Attempting to recreate consistent bed substrates for each test would also be difficult given the volume of sediment required and the difficulty in creating different sand-gravel beds with exactly the same properties. Clay particles were not observed to deposit in appreciable quantities below the armor layer

of the sand-gravel bed tests. Because of this only the armor layer was cleaned between tests. This was done by gently disturbing the surface grains of the armor layer while water was flowing at low speed in the flume. This caused the deposited clay to entrain from the bed without entraining large quantities of sand. The flume water was then drained and the process repeated with clean water until no sediment entrained from the bed. This was the only effective way to clean the sand-gravel bed while causing minimal changes to the properties of the bed.

3.1.5 Mass Flux to the Bed

There is no practical way to measure the accumulation of clay mass on any of the bed types examined in these experiments. The mass flux across the sediment-water interface was therefore quantified by measuring concentration change in the water column with time and coupling this to a theoretical model for sediment deposition and resuspension within the flume (discussed in detail below). Clay concentration within the water column was measured using two optical backscatter sensors (OBS 3+), one near the upstream end of the test section and one near the exit of the test section. Data was compiled on a Campbell Scientific CR200X data logger. Both OBSs were calibrated simultaneously in a mixture of kaolinite clay which was kept in suspension by a mixer. The calibration range of concentrations was from 0 mg/L to 1000 mg/L, well within the expected range of concentrations in the experiments.

The concentration time series was begun once the flume system was well mixed for a given test run. Well mixed was determined by the time at which both OBS readings were

approximately the same, showing consistent concentration along the length of the flume. The time scale of mixing within the system was also measured as the time to steady-state readings on a conductivity meter when a pulse of saltwater was added to the system in identical fashion. Salt tracer tests further showed that there was a very slow exchange between surface and pore water, Figure 3.5. This exchange was limited to the first hour of the tracer tests. The pore water constitutes approximately 4% (Sand-Gravel Bed) to 6% (Gravel Bed) of the total system volume. The slow and limited duration of the exchange indicates that much of the observed concentration decay in the water column was cauesd by sediment settling and not surface-pore water exchange. The data logger recorded suspended sediment concentration measurements every six seconds. This data was then reported as one minute time averages. The standard deviation within these one minute averages ranged from 0.01 mg/L to 2.56 mg/L with a mean standard deviation of 0.72 mg/L. The OBS meters have an accuracy of $\pm 2\%$ or 1 mg/L, whichever is higher.

Concentration measurements were taken at a height of 2.54 cm from the flume bed. A preliminary set of experiments were run to ensure that placing the OBSs at this height would yield repeatable and representative concentrations of the entire depth. In this set of preliminary experiments, concentration data was collected at a series of vertical locations in the water column over the range of discharges used in the primary experiments. The data all show that the suspended sediment can be characterized as "well mixed" over the vertical; implying that a measurement taken at 2.54 cm from the bottom of the bed is representative of the depth averaged concentration. Rouse number calculations further support this

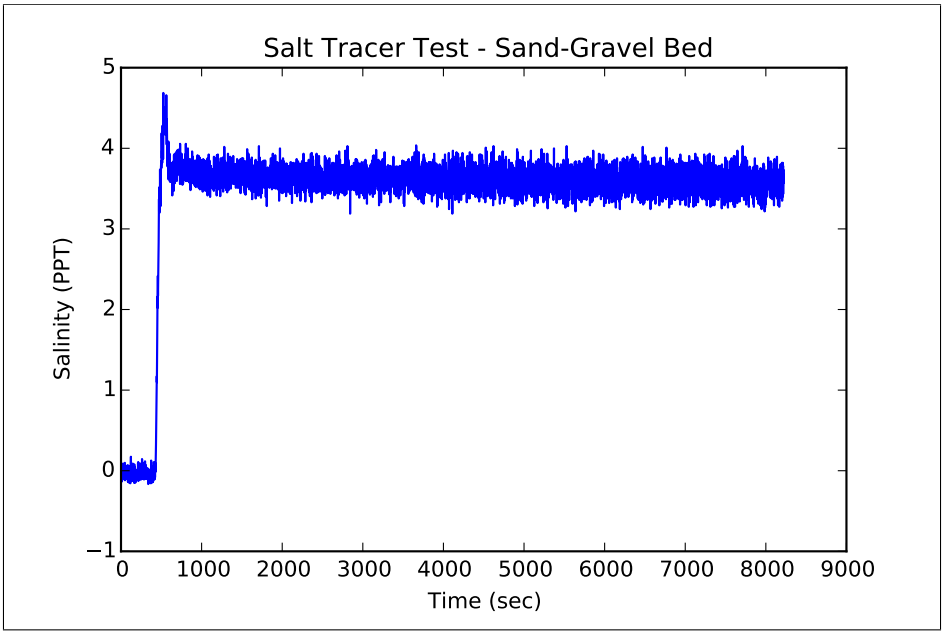

Figure 3.5: Characteristic salt tracer test over sand-gravel bed.

conclusion. P values for the range of sediment sizes measured in suspension (3.3 to 36.6 μm) ranged from 2×10^{-9} to 2.4×10^{-7}. The observed concentration difference between the upstream and downstream OBS was within the error tolerance of the instrument. That is, spatial change in concentration along the length of the test section was so small that it was not measurable with the OBS.

3.1.6 Suspended Particle Sizes

Suspended clay aggregate size was measured using a floc imaging system. Samples of suspended sediment were collected near the bed using a large-diameter (8 mm) pipette. The sample was then gently released into a back lit settling column where the suspended aggregates were photographed with a Point Grey high resolution camera. The camera uses a 2080x1552 pixel progressive scan CMOS sensor that, when combined with a set of 2x ob-

jective optics, yields a resolution of 1.267 μm per pixel. Characteristic sizes of suspended sediment were determined from these pictures using ImageJ image analysis software. This software uses sharp gray scale gradients to determine the extent of the particle boundaries and produces images showing the measured particle outlines (Figure 3.6). It then assigns size characteristics to the given particles based on the number of pixels within the limits of the particle. The ImageJ settings were altered for each test until a good fit between the observed particles and the software determined particle outlines matched. The pixel data was then converted to a volume size distribution with a conversion algorithm in Python.

Samples of suspended aggregate size were collected over the entire duration of each experiment. The frequency of sampling was higher at the beginning of each test (5 minute intervals) and slower at the very end of the test (30-60minutes) to account for the rapid settling of larger aggregates early in the test. The particles which remained in suspension fined over the duration of the test. Since particle settling velocity is dependent on particle size this indicates that the characteristic settling velocity of the particles in suspension will decrease with time.

3.2 Theoretical Framework

The theoretical framework used to interpret the experimental results is based on a mass balance of sediment in the water column. A primary component of the framework is the assumption that reductions in concentration within the water column are due to deposition of sediment either within the flume test section (i.e., the bed) or somewhere within the

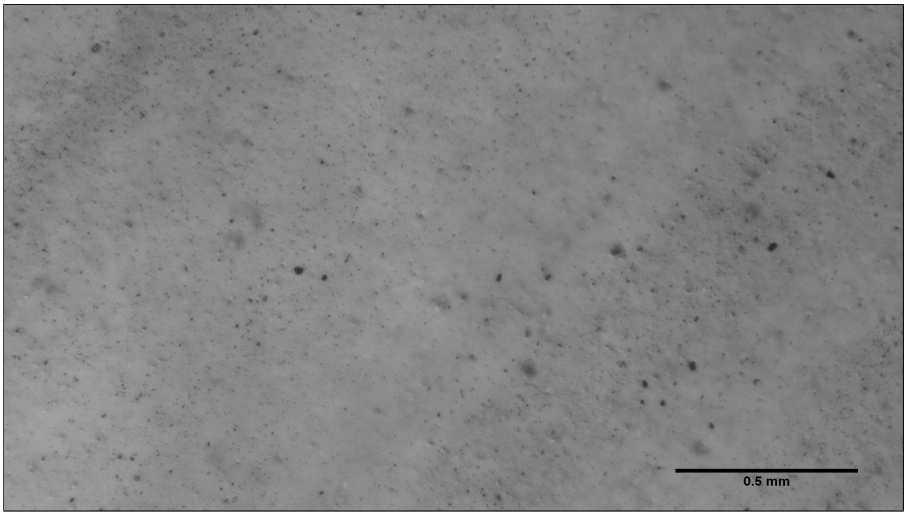

(a) Image of clay particles drawn from suspension at the beginning of Gravel Bed Test 6

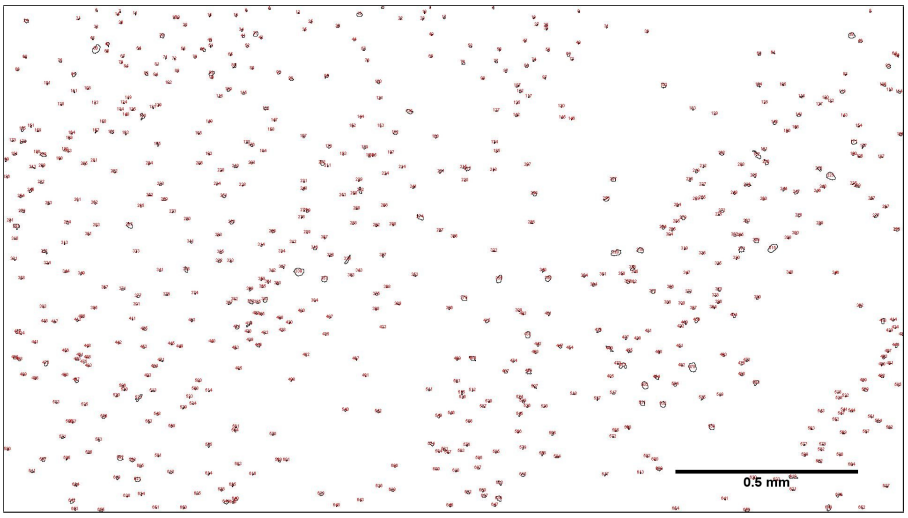

(b) ImageJ determined outline of particles observed in Figure 3.6a

Figure 3.6: Comparison of observed suspended clay particles and the ImageJ measured particles

flumes recirculation system (i.e., the system). To begin, consider the following 1D mass conservation equation for suspended sediment in a river written for conditions away from a diffuse front:

$$\frac{\partial(AC)}{\partial t} + \frac{\partial(AUC)}{\partial x} = \frac{\partial}{\partial x}\Big(AD\frac{\partial C}{\partial x}\Big) + b\Big(E_b - D_b\Big) \tag{3.3}$$

where A is the cross sectional flow area, C is concentration (mass or volume) of suspended sediment, D is the dispersion coefficient, E_b is an erosive flux and D_b is a depositional flux across the sediment-water interface. This is illustrated in Figure 3.7. Dimensionally E_b and D_b are expressed as [L]/[t] in volume units and [Mass]/[L^2 t] in mass units. Given that the flume cross section is rectangular and prismatic the cross sectional area can be taken as $A = bh$. Additionally, since we consider the time after full mixing (no strong diffuse front present), and because the change in concentration along the length of the cross section was not quantifiable, the concentration gradient $\partial C/\partial x$ is negligible and the dispersive term can be removed. Equation 3.3 can further be simplified by assuming the spatial change is small relative to the time change in C over the time scale of interest. This is a valid assumption for the experimental setup because the difference between the concentration readings from the upstream and donwstream OBSs was within the error tolerance of the two instruments.

$$\frac{\partial C}{\partial t} = \frac{1}{h}\Big(E_b - D_b\Big) \tag{3.4}$$

The net result of the erosive and depositional fluxes can be taken as a combined inter-

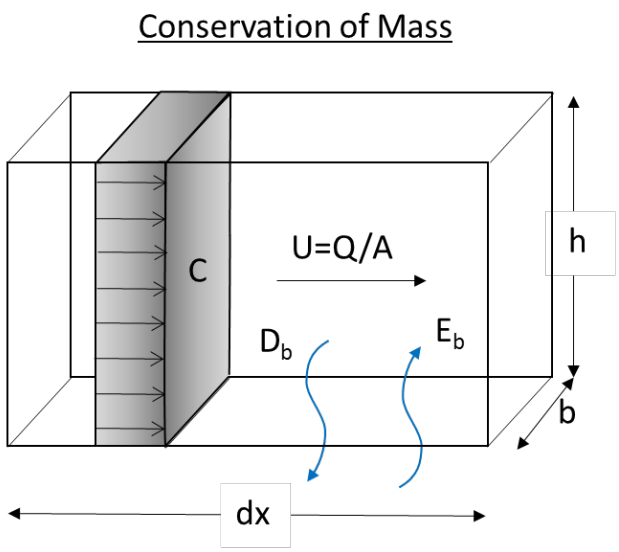

Figure 3.7: Wash Load Conceptual Model

action term N_{ss} which describes the net source/sink of wash load across the sediment-water interface.

$$E_b - D_b = N_{ss} \tag{3.5}$$

In classic sediment transport modeling of sand-size sediment, deposition is modeled as the product of the settling velocity and the near bed concentration (which is the same as the depth averaged concentration in fully mixed conditions):

$$D_{b,m} = w_s C \tag{3.6}$$

The erosion term is then taken as the product of the settling velocity and an erosion rate equation (which is equal to the near bed concentration under conditions of steady state):

$$E_{b,m} = w_s E_s \tag{3.7}$$

where E_s is the erosion rate (Garcia, 2008).

For our purposes, we combine erosion and deposition into a single term and take N_{ss} to be a function of the settling velocity, w_s, the concentration, C, and some condition dependent constant, α_1:

$$N_{ss} = \alpha_1 w_s C \tag{3.8}$$

Hence,

$$\frac{\partial C}{\partial t} = \frac{1}{h}\alpha_1 w_s C \tag{3.9}$$

In this way, α_1 represents the fraction of material available to deposit that actually does so at any instant in time.

Equation 3.9 assumes that the flow is always in contact with the bed. This assumption is not valid for the experimental setup used in this study given that much of the total volume of fluid and sediment is contained with in the recirculation system. That is, when a packet of fluid is not in the flume test section, it is in contact with the rest of the flume system which includes the downstream tank, the pump, pipes, and the flume head box. Settling of sediment can occur in several of these locations, primarily the downstream tank and the head box. Because of this, the model must account for contact time between any given packet of fluid and the bed versus the rest of the system, and it must account for any deposition that occurs outside of the test section.

Because sediment laden fluid is only in contact with the bed for a fraction of the system cycle time, a time adjustment factor is used to correct for contact time with the bed. This

time factor is also used to account for deposition within the system when the fluid is not in contact with the bed. Time will be adjusted by using the system discharge and the relative volume of fluid in the channel and total system. The volume within the flume test section is given by $V_{flume} = bhL$, where L is the length of the flume. The total volume within the entire flume system is referred to as the system volume, V_{sys}. Using these terms and the channel discharge (Q) we can define two important measures of time. The turnover time,

$$T_T = \frac{V_{sys}}{Q} \tag{3.10}$$

and the flume test section contact time, T_c:

$$T_c = \frac{V_{flume}}{Q} = \frac{bhl}{bhU} = \frac{L}{U} \tag{3.11}$$

The fraction of time for a given packet of fluid in contact with the bed can be taken as,

$$\beta = \frac{T_c}{T_T} \tag{3.12}$$

The fraction of time a packet of fluid is in contact with the rest of the system can be taken as $(1 - \beta)$. We can include these terms into the governing equation with an added term for the source/sink in the flume system (N_{ss-sys}),

$$\frac{\partial C}{\partial t} = -\frac{\beta}{h}\alpha_1 w_s C + \frac{1}{[L]}(1-\beta)N_{ss-sys} \tag{3.13}$$

where L is a characteristic length scale to ensure dimensional homogeneity. This length is difficult to quantify as an independent measure as it would have to describe a characteristic length of the flume system outside the channel. This is difficult because there are several areas where deposition can occur (i.e., the downstream tank, headbox, etc.) which are vastly different in size. In order to keep the system decay portion of the model dimensionally consistent it is modeled with settling velocity and combined with the length scale and N_{ss-sys} as a system capture term.

$$\frac{1}{[L]}N_{ss-sys} = -w_s\alpha_* C \tag{3.14}$$

where α_* is the system capture term and has units of [-]/[L]. This system decay term, used within the governing equation, forms an equation which takes into account settling in the entire flume system as measured by the OBSs described in the experimental procedure:

$$\frac{\partial C}{\partial t} = -w_s C\Big[\frac{\beta}{h}\alpha_1 + (1-\beta)\alpha_*\Big] \tag{3.15}$$

Solving this equation for concentration as a function of time can be done through the separation of variables as follows:

$$\frac{\partial C}{C} = \Big[-\frac{\beta}{h}\alpha_1 w_s - (1-\beta)\alpha_* w_s\Big]\partial t \tag{3.16}$$

$$\ln(C) = \Big[-\frac{\beta}{h}\alpha_1 w_s - (1-\beta)\alpha_* w_s\Big]t + C_1 \tag{3.17}$$

where C_1 is a constant of integration, which is related to the initial concentration at $t = 0$, as

$C_1 = \ln(C_o)$. Substituting this initial condition into Equation 3.17, rearranging and raising both sides to e gives:

$$C(t) = C_0 e^{-w_s\left[\frac{\beta}{h}\alpha_1 + (1-\beta)\alpha_*\right]t} \tag{3.18}$$

This equation assumes that settling velocity and the decay terms (α_* and α_1) are constants and that they represent the amount of sediment settling within the system and in the bed, respectively.

It has been shown in the literature (Lau and Krishnappan, 1992, 1994; Haralampides et al., 2003), and in the experiments of this study, that large suspended particles settle out of suspension faster than smaller particles. If the size of the material in suspension decreases with time, one would expect the settling velocity of the suspension to also decay with time. Given this, it is more physically meaningful to write a mass balance equation for each size fraction, and then to sum the resulting concentration time series across all size fractions to obtain the total concentration time series. Such an approach is followed here using Equation 3.19 as the mass balance equation for size fraction, i:

$$C_i(t) = C_{oi} e^{-w_s\left[\frac{\beta}{h}\alpha_{1i} + (1-\beta)\alpha_{*i}\right]t} \tag{3.19}$$

If one divided the overall concentration decay into bins based on size classes of the suspended sediment the concentration fraction of larger sediments would decay faster than that of the smaller sediments. This effectively takes into account the reduction of settling velocity over time without introducing a time dependent term.

Since settling velocity and concentration have been divided by size fraction of sediment, α_* and α_1 cannot be constant. Larger particles may have a higher probability of deposition whereas smaller particles a lower probability of deposition and greater likelihood to re-suspend. These terms must then be scaled in order to account for preferential deposition or entrainment based on size class. To account for this, the alpha constants are multiplied by a scaling term, Θ_i, which is taken as the various sediment size fractions normalized by the largest size fraction.

$$\Theta_i = \frac{D_i}{D_{max}} \tag{3.20}$$

where D_i represents the bin centered size of each of the size fractions comprising the suspended sediment and D_{max} is the largest of these size fractions. In effect Θ_i is a series of values which correspond to each size class with the largest value (1) associated with the largest size fraction and the smallest value ($\ll 1$) associated with the smallest size fraction. At first glance one might think that the inclusion of Θ_i assumes that the largest size fraction will completely settle out of suspension. This, however, is not the case. One can think of Θ_i as a coupled term with α_1 and α_* which are constants describing the holistic capture of sediment by the bed, i.e., $\alpha_{1i} = \Theta_i \alpha_1$. This combined term accounts for the faster decay of sediment to the bed for the larger size fraction and slower decay for the smaller size fractions.

$$C_i(t) = C_{0,i} e^{-w_{s,i}\Theta_i \left[\frac{\beta}{h}\alpha_1 + (1-\beta)\alpha_*\right]t} \tag{3.21}$$

with,

$$C = \sum_{i=1}^{N} C_i \tag{3.22}$$

This model (Equations 3.21 and 3.22) only relies on the initial size fractions of the suspended sediment and the system and bed decay terms. Translation of this equation to the field could be accomplished by letting $\beta = 1$ such that the flow is always in contact with the bed. The Equation would then describe the decrease in suspended sediment concentration within a block of river water within a moving frame of reference.

4 Results

The results of the experiments show the temporal and spatial interaction of wash load sediment with different bed types and under varying hydraulic conditions. The processing of the observed concentration data began with the determination of the time correction factor (β) to ensure proper scaling of the concentration decay with respect to the time that the flow was in contact with the bed. Following this, the size distributions of the suspended sediment over time were determined. The initial size class and its change over time drove the development of the mass decay mode discussed previously. The initial size class also defines the Θ_i term. The background decay was characterized through an application of a system decay only model (Equation 4.2) to acrylic bed tests with no bed deposition. The quantification of these terms then made it possible to fit the theoretical model (Equations 3.21 and 3.22) to the data observed in the experiments, quantifying the mass captured by the bed in the α_1 term. Trends in α_1 with shear stress, bed type, or initial concentration would indicate the impact of these factors on the interaction of wash load with different bed types. Visual inspection of clay on the bed surface and/or within the substrate was used to determine the spatial distribution of sediment within the bed. The observed concentration response during the entrainment phases was used to determine the depositional flux response

to higher shear stresses.

4.1 Time Correction Factor, β

The time correction factor is slightly different for each test run and for each increase in discharge during the entrainment phases. As discharge increases, the depth of the water column and the volume in the flume channel both increase. This means that at higher discharges there is greater contact time with the bed relative to the rest of the system. The time correction factor across all tests ranges from 0.12 to 0.33. This term does not manifest itself when comparing the raw data but will greatly affect the regressed α_1 values. That is, raw data trends may appear similar or different but the fundamental decay rate may differ because the contact time with the bed was different for tests with different discharges.

4.2 Trends in the Suspended Particle Size Distribution with Time

As discussed earlier the suspended sediment particles greater than 5 μm in diameter were imaged with a high resolution camera and the images were processed using ImageJ software. The size data were then converted to volume dimensions assuming that the particles were spherical. Given the mildly cohesive nature of kaolinite, the recirculation of particles through a centrifugal pump, and the sampling of sediment through a pipette, one would not expect any large, loosely packed flocs to show up in the images. Observations from the images were consistent with this assumption in that no large loosely packed flocs were observed. However, the images did show that the more densely packed aggregates of various sizes

did form. The initial size distribution of these aggregates (between 10 to 40 μm) did not change dramatically over tests of different bed types or initial bed shear values (Figure 4.1). However, in all cases, the size distribution of suspended material did fine over the coarse of each experiment.

Given their similarity, the size distributions were combined to produce a single average initial particle size distribution that was representative of all tests. Generating the representative distribution involved creating seven bin sizes and placing the corresponding frequency of observations of the given size classes from each test into the corresponding bin. A comparison of all observed size distributions and the representative size distribution is shown in Figure 4.1. Seven bins were used in order to keep calculations minimal when calculating model results. Given the organization of concentration calculations by size fraction any number of bins could be used when applying the model.

As stated previously, the size distribution of the suspension fined with time. This can be attributed to the larger particles settling out of suspension faster than the smaller particles. The reduction in size of various size fractions over time can be seen in Figure 4.2a. All size statistics linearly decrease with the logarithm of time, but the size statics of d_{84} and d_{90} decay at a faster rate than d_{16} (Figure 5.3b). This trend clearly indicates that larger particles are removed from the suspension faster than smaller particles. A best fit log-linear line has been fit to the data in Figure 4.2b. These equations take the general form of:

$$D_i(t) = \eta \ln(t) + D_{0,i} \tag{4.1}$$

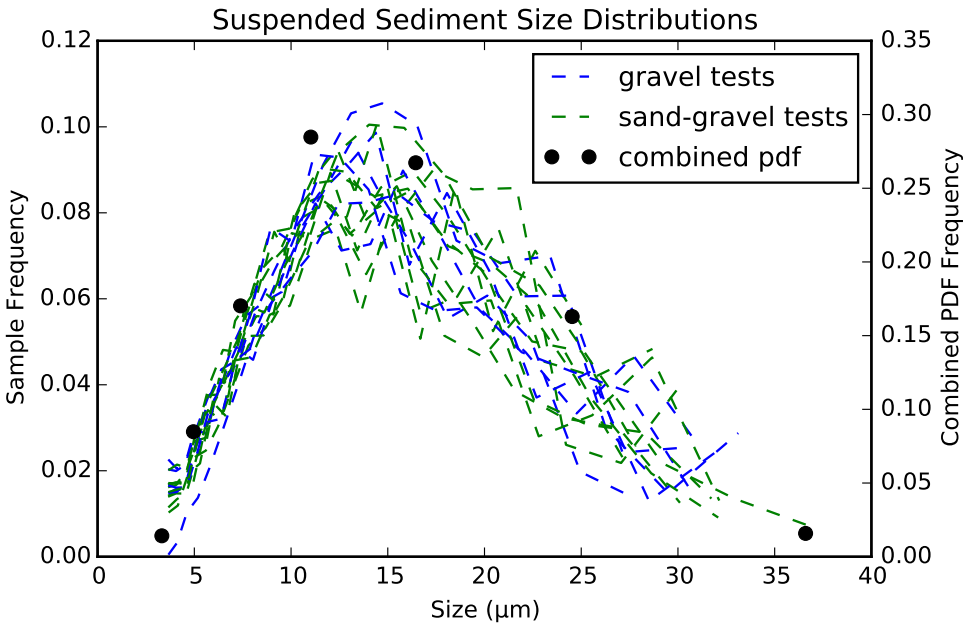

Figure 4.1: Observed suspended sample size distribution and the combined representative suspended sediment size distribution.

where $D_i(t)$ is the diameter of a suspended sediment particle of size fraction i as a function of time,η is the decay rate, and $D_{0,i}$ is the initial diameter of the given size fraction. This relationship also indicates that the suspension averaged settling velocity will decay with time.

4.3 The Deposition Phase: Loss of Mass from the Water Column

In this next section, the changes in the suspended sediment concentration during the deposition phase of each experiment are used to determine the amount of sediment that deposited within the flume test section for each bed type, shear velocity, and initial concentration. To do this, the theoretical model (Equations 3.21 and 3.22) is calibrated using the OBS time series data. Equation 3.12 is used in conjunction with the OBS data to allow for the contact

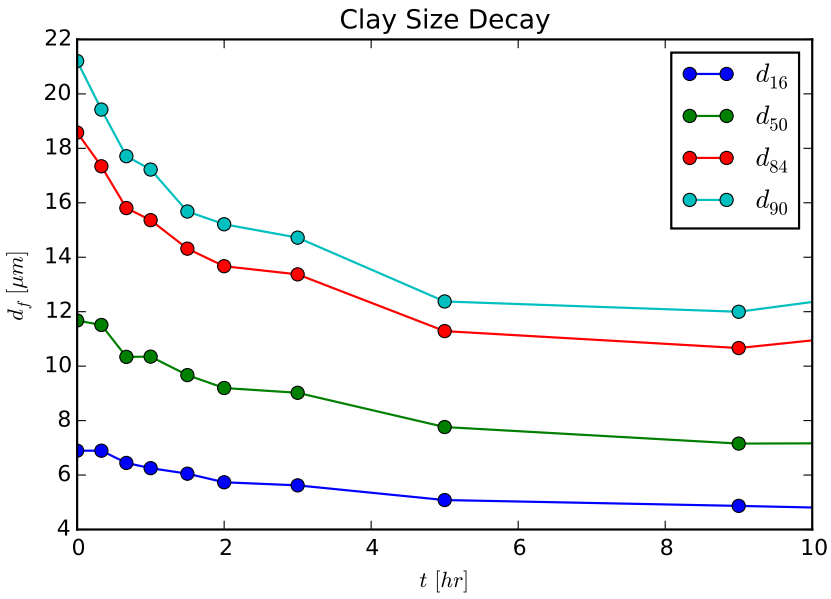

(a) Suspended sediment size decay with time

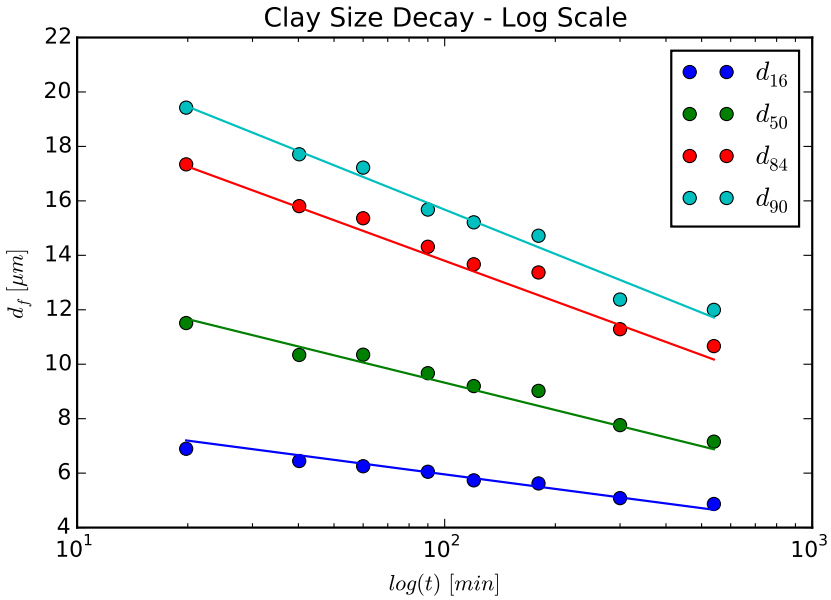

(b) Suspended sediment decay, log scale

Figure 4.2: Size distribution of the combined seven and 20 bin pdfs.

time correction and loss of mass to the recirculation system to be accounted for. Results from the entrainment phase of each experiment will be presenting in Section 4.4.

4.3.1 Background Mass Decay in the Flume System

To use the concentration data to determine the α_1 factor for each bed type and flow condition, one must first quantify the system decay term α_*. The quantification of α_* was done by using concentration decay data for acrylic bed tests in the presence of high bed shear stress. During these tests low speed streaks and, in some instances, very small bedforms were present. The streaks formed during the first minutes of the experiment and did not grow or shrink over the duration of the tests. In some of these tests, small bedforms developed in the wake of the Vectrino or OBSs. These bedforms remained small and eventually migrated downstream and out of the channel without growing or shrinking in size. This indicates that there was bedload movement of clay aggregates over the smooth boundary, but that depositional and entraining forces were at steady state. The long term decay observed during these tests can thus be attributed to decay within the recirculation system outside of the flume test section. In this case, α_1 was set to zero, resulting in the following time-dependent model for C based only on settling within the tail tank, headbox, and recirculation piping:

$$C_i(t) = C_0 e^{[w_{si}\Theta_i(1-\beta)\alpha_*]t} \tag{4.2}$$

Equation 4.2 was used in conjunction with the OBS data, initial particle size distribution, the time correction factors β, and the Θ_i values to determine, through regression, an α_* value for

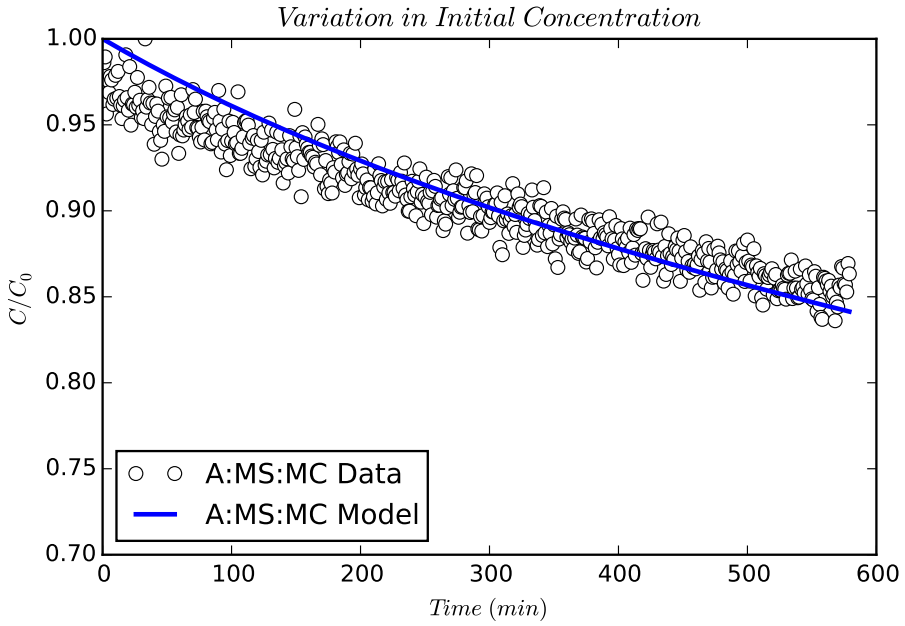

Figure 4.3: Best fit of system decay model (Eq. 4.2) to observed data from Test A:MS:MC.

Tests A:HS:LC, A:MS:MC, A:HS:MC, and A:HS:HC. Note that the Stokes settling velocity equation was used to determine the w_{si} values for all size fractions since the diameters were all less than 40 μm. The α_* resulting from this procedure were nearly the same for all test, with an average $\alpha_* = 0.138$ m^{-1}. Figure 4.3 shows an example of the model fit to the data for smooth wall run 5.

4.3.2 Mass Accumulation in the Bed

The average α_* value calculated in the previous section was used in conjunction with the theoretical model and OBS data in the cases where there was deposition of clay within the flume test section to quantify the loss of sediment to the bed. Using the same α_* value in the cases where a sediment did accumulate in the flume test section is reasonable given that

the flow in the recirculation system (tail tank, head box, and recirculation piping) did not change dramatically over the various test conditions.

The deposition factor, α_1, was determined by regression using the β values specific to each test, the OBS concentration time series, and the theoretical model for C (Equations 3.21 and 3.22). In the calculations, the constant α_* was used along with the measured depth, h, the characteristic initial particle size distribution, the previously defined Θ_i values, and the w_{si} for each size fraction as given by the Stokes settling equation. The final α_1 values obtained from model fitting are presented in Table 4.1. The best fit parameters, R^2 presented in Table 4.1 were calculating by transforming Equation 3.21 to linear form by taking the natural log of both sides of the equation prior to calculating the goodness of fit. Example fits of the model to observed data are shown in Figure 4.4 for each of the separate bed types.

4.3.3 Bed Type Trends

The trend in concentration decay across the various bed types is stark. In general, mass flux to the bed decreases with decreasing pore space in the bed (Figure 4.5). The α_1 values for the acrylic bed tests are orders of magnitude lower than those of the gravel and sand-gravel bed tests. This is logical as the acrylic bed has no pore space for grains to settle and are thus completely exposed to the entraining properties of the near bed flow. The highest shear stress runs of the acrylic bed tests were also used to define the system concentration decay as deposition in the test section during these experiments was negligible. The difference between the gravel and sand-gravel bed tests is smaller than the differences between these

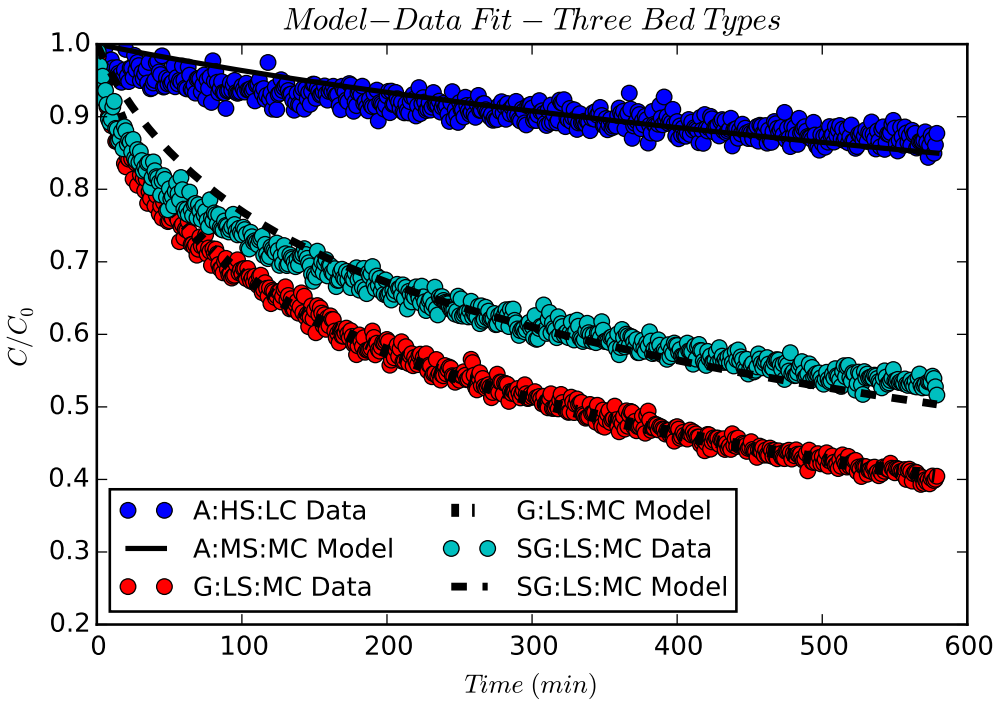

Figure 4.4: Model-Data relationships over the three different bed types.

tests and the acrylic bed tests. One can best examine the impact of the bed type on the trapping of wash load by examining the α_1 values obtained for different bed conditions at the same, or nearly the same, shear velocity.

The gravel and acrylic bed tests are compared at a shear velocity of $u_* = 0.0168$ m/s and will be compared to the sand-gravel tests at $u_* = 0.0191$ m/s (Figure 4.5). The α_1 values for characteristic gravel (G:LS:MC), sand-gravel (SG:LS:MC), and acrylic glass (A:HS:LC) tests are 0.433, 0.397, and 0.00101, respectively. The difference between the representative gravel and sand-gravel bed tests is 8% ($\Delta\alpha_1$=0.036) and well within the same order of magnitude. The difference between the porous bed tests (gravel and sand-gravel) and the acrylic bed test are 99% and cover almost two orders of magnitude.

Test	α_1 (m^{-1})	U_* (ms^{-1})	C_0 (mgL^{-1})	R^2
A:LS:LC	7.21E-02	0.0106	101	0.82
A:MS:LC	4.50E-02	0.0154	84	0.56
A:HS:LC	1.01E-03	0.0168	84	0.63
A:LS:MC	6.90E-02	0.0111	191	0.76
A:MS:MC	3.74E-06	0.0152	195	0.83
A:HS:MC	4.70E-04	0.0181	177	0.65
A:LS:HC	9.44E-02	0.0110	397	0.42
A:MS:HC	2.54E-02	0.0151	378	0.57
A:HS:HC	3.25E-04	0.0177	403	0.57
G:LS:LC	0.617	0.0168	93	0.99
G:MS:LC	0.746	0.0206	87	0.99
G:HS:LC	0.604	0.0233	88	0.99
G:LS:MC	0.433	0.0168	199	0.99
G:MS:MC	0.573	0.0206	192	0.99
G:HS:MC	0.731	0.0233	176	0.99
G:LS:HC	0.450	0.0166	411	0.98
G:HS:HC	0.727	0.0230	396	0.98
G:MS:HC*	0.604	0.0345	393	0.99
G:VHS:LC	0.610	0.0333	88	0.99
G:VHS:MC	0.490	0.0333	192	0.98
G:VHS:HC	0.551	0.0333	363	0.98
SG:HS:LC	0.397	0.0241	93	0.97
SG:LS:LC	0.470	0.0191	87	0.92
SG:MS:LC	0.416	0.0221	88	0.94
SG:LS:M	0.397	0.0192	199	0.93
SG:MS:MC	0.307	0.0221	192	0.95
SG:HS:MC	0.314	0.0241	176	0.96
SG:LS:HC	0.429	0.0191	411	0.84
SG:MS:HC	0.351	0.0221	396	0.87
SG:HS:HC	0.410	0.0241	393	0.83
SG:VHS:LC	0.326	0.0283	88	0.92
SG:VHS:MC	0.233	0.0283	192	0.97
SG:VHS:HC	0.239	0.0283	363	0.96

Table 4.1: α_1 values for the acrylic, gravel, and sand-gravel bed tests
P - Acrylic Bed. G - Gravel Bed. SG - Sand-Gravel Bed.

Upon review of Figure 4.5 one might consider these differences muted given that the visual difference between the gravel and sand-gravel tests seems only slightly smaller than

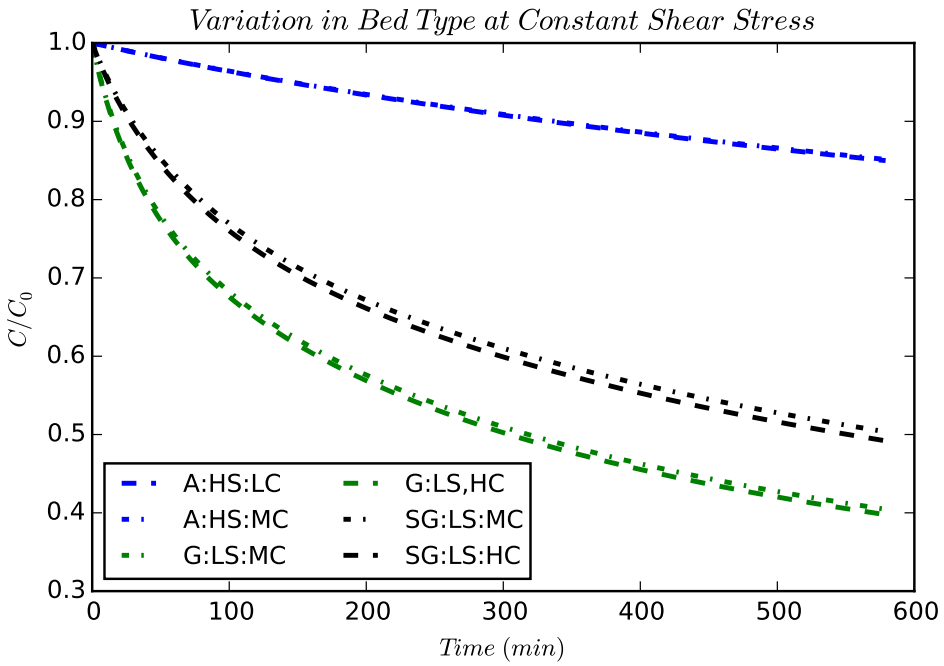

Figure 4.5: Comparison of different bed types over consistent bed shear stresses.

the change between the sand-gravel tests and the acrylic bed tests. One should note that these curves account for bed and system decay and that the acrylic bed tests examined had almost no bed deposition. The concentration in the flume system for the acrylic tests is much higher than the porous bed tests in which there was significant bed deposition. Equation 3.15 shows that the effect of α_1 and α_* are dependent on the concentration in the test channel and system. In comparing the acrylic bed and porous bed tests, one must consider that the higher concentration in the former causes the effect of α_* to be greater (Figure 4.6). Once a porous bed is present the effect of the background decay is highly diminished because of the reduced concentration in the system.

Shear stress and bed type have a distinct effect on the decay rate. When considering porous beds comparable to those found in natural streams the bed type has a larger impact

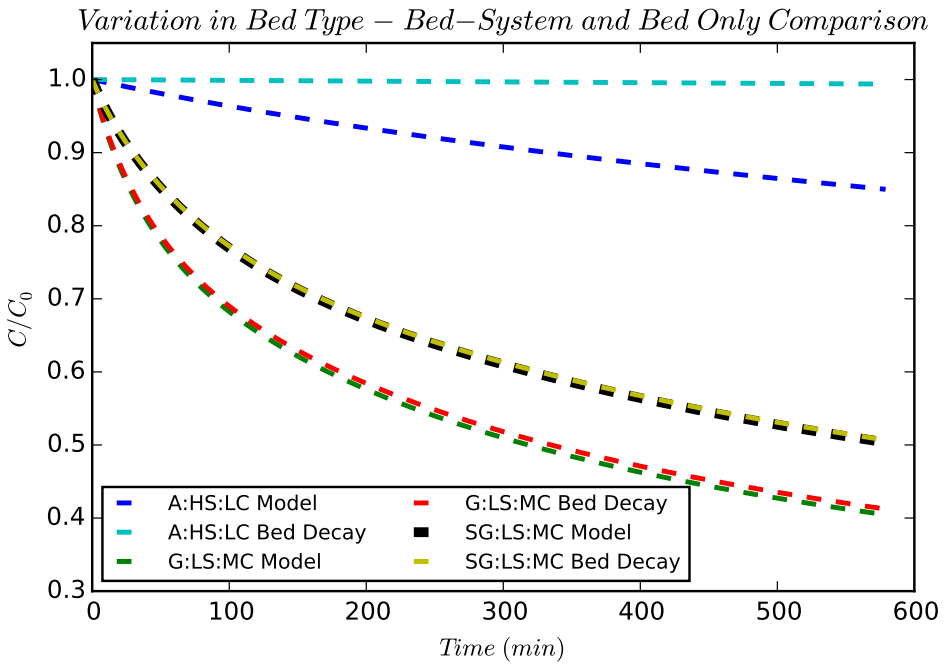

Figure 4.6: Difference between bed/system and bed only decay.

on the decay rate than changes in shear stress for conditions in which the bed surface material is not in motion.

4.3.4 Initial Concentration Trends

Results in the literature indicate that fine sediment decay rates are invariant with initial concentration (Lau and Krishnappan, 1994; Mehta and Partheniades, 1975). Similar results were observed in this study (Figure 4.7). When comparing normalized decays of different concentrations the decay curves and final concentrations appear very similar for the same bed shear condition despite different starting concentrations. The α_1 values were not exactly the same for each bed shear condition and no trend of variation was found when examining changes in initial concentration. This seems to indicate that the difference between these

results is likely not a trend, but rather an artifact of experimental variability. The comparison given in Figure 4.7 includes the 200 mg/L and 400 mg/L tests only. The variation in the results experienced in the Sand-Gravel Bed Tests was greater than experienced in the Gravel Tests. This may have been a result of the difficulty in re-setting the sand-gravel test without disturbing the substrate. The results which were most consistent with results in the literature were tests over different concentrations at $u_* = 0.0241$ m/s and $u_* = 0.0283$ m/s which are also presented in Figure 4.7. The trends within the acrylic bed tests were generally more consistent, which is understandable given the consistency over which it is possible to re-set the bed conditions.

The α_1 values associated with similar shear stress with different initial concentration values were very similar. When comparing the gravel test α_1 values for the tests compared in Figure 4.7a numerically they are within 0.55-3.9% of each other. The compared sand-gravel bed tests show α_1 values which are within 2.51-8.06% of each other. Of the acrylic glass tests compared in Figure 4.7c the α_1 values are within 1.34-3.69% of each other. Though some of these values may be greater than 5% apart several of them indicate no change between the decay term given changes in initial concentration. This is more the case for higher concentration and higher shear tests as compared to the lower shear/concentration tests which tend to be more variable.

The implication of these results is twofold. First, it indicates that the fractional transfer of suspended mass to the bed is independent of starting concentration for a given bed shear stress. This shows that our results are similar to those shown in the literature. Secondly,

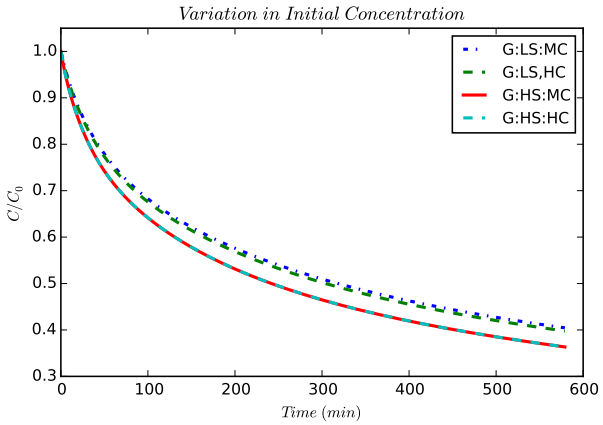

(a) Decay rate over the gravel bed at constant shear

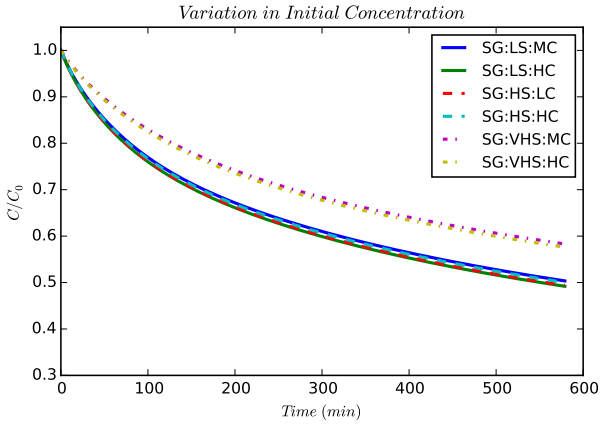

(b) Decay rate over the sand-gravel bed at constant shear

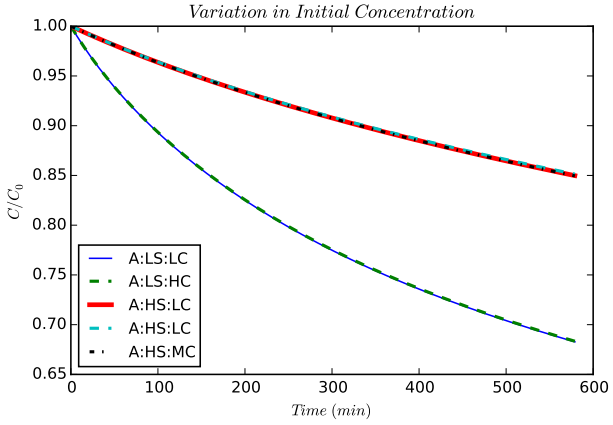

(c) Decay rate over the acrylic bed at constant shear

Figure 4.7: Mass decay rate with differing starting concentrations at the same bed shear stress.

it shows that this trend appears to hold for beds of different sediment compositions. That is not to say that the decay rate is the same for different bed compositions, but that for a given bed composition the decay rate at a given shear stress is independent of the starting concentration.

4.3.5 Shear Stress Trends

Data from the experiments showed that α_1 is dependent on the bed type, but not dependent on the initial concentration of the suspension. Here the dependence of α_1 on u_* is examined. For simplicity in presentation, an examination will be made of a single starting concentration over the range of shear stresses examined in this study. Given the competition between depositional, w_s, and erosional, u_* effects, I hypothesized that increases in u_* would cause α_1 to decrease. An examination of how concentration decay changes as a function of shear stress for the different bed states is shown in Figures 4.8, 4.9, and 4.10.

The acrylic bed tests (Figure 4.8) show a significant change in the concentration decay with changes in bed shear stress. This change is much more pronounced than that shown in the gravel and sand-gravel bed tests (Figures 4.9 and 4.10). The comparatively greater impact of bed shear stress on mass flux from the water column for the acrylic glass tests is logical as there is no substrate below the acrylic bed in which depositing sediment can settle or hide. Sediment which deposited on the bed surface could be more easily entrained by increases in shear stress. Also note that the acrylic bed tests almost reach equilibrium concentration values whereas the gravel and sand-gravel bed tests do not. This indicates

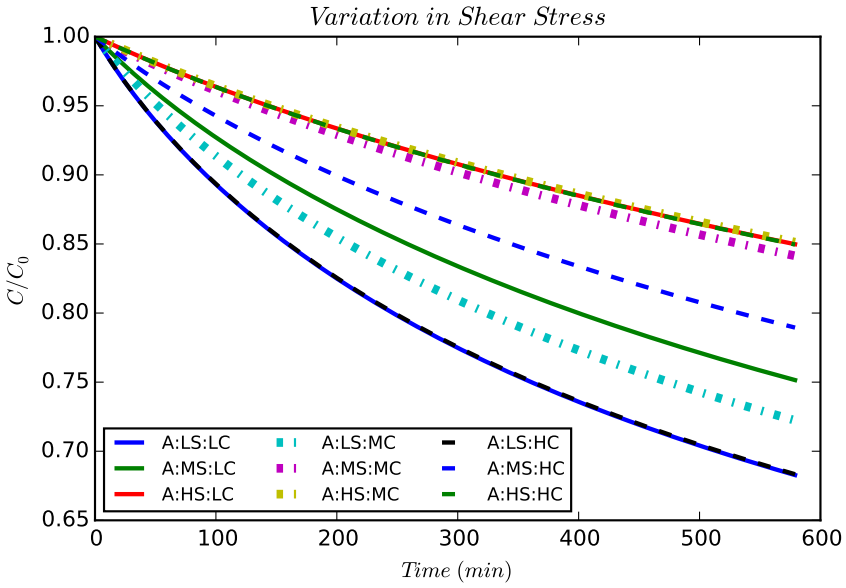

Figure 4.8: Changes in concentration decay over time with changes in shear stress over the acrylic bed. Note that at certain shear stresses the decay becomes consistent indicating that at some point only background decay is governing the decay rate

that the tests over the acrylic bed might approach equilibrium balance between deposition and erosion or re-suspension.

The gravel and sand-gravel bed tests do not approach equilibrium and tend to continually deposit over time. Furthermore, the decay trends in these tests show much less sensitivity to changes in shear stress (Figures 4.9 and 4.10). A comparison of the α_1 values between tests of different shear shows a general trend of decreasing α_1 with increasing u_*. This is most apparent in comparing the lowest and highest bed shear tests. However, small shear changes between the highest and lowest values do not consistently fit the aforementioned hypothesis. These variations are similar to the experimental errors observed when comparing trends of initial concentration in Section 4.3.4. These results indicate that there is a general trend of decreasing mass flux with increasing bed shear stress. It also indicates

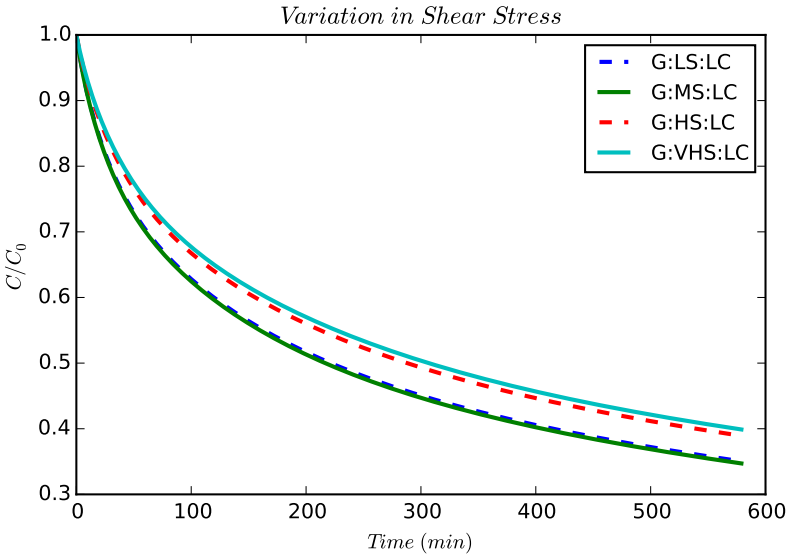

(a)

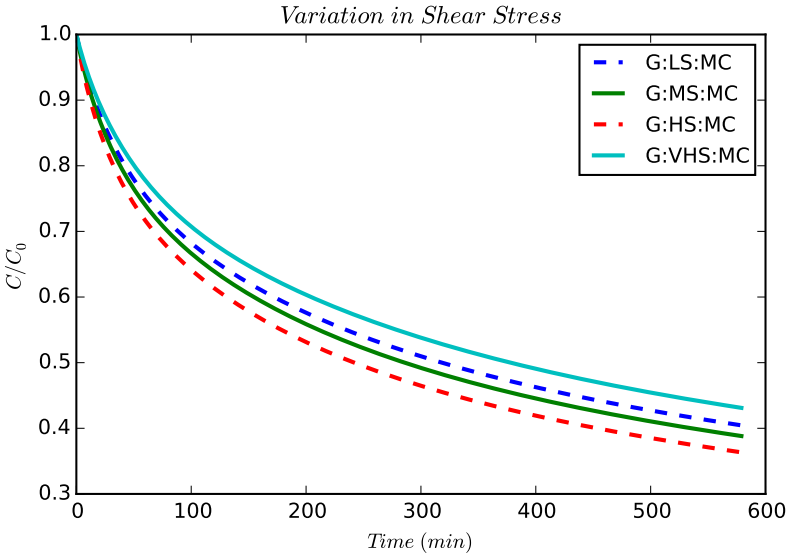

(b)

Figure 4.9: Changes in concentration decay over time with changes in shear stres over the gravel bed

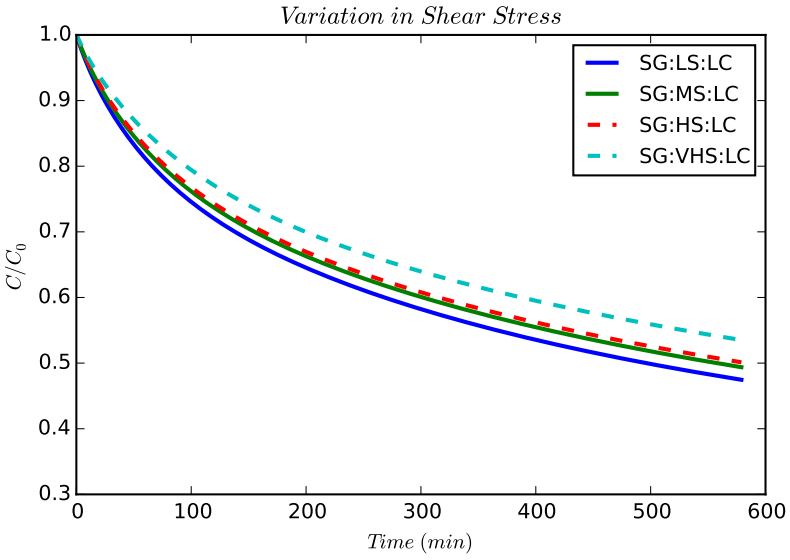

(a)

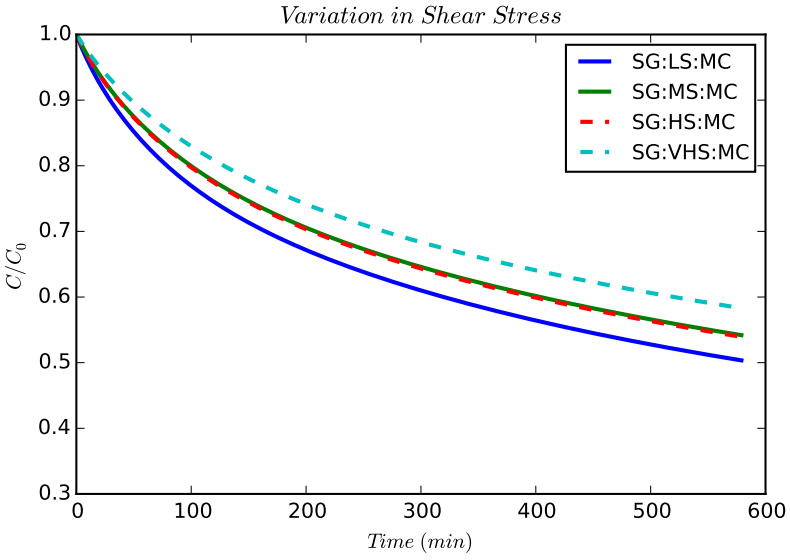

(b)

Figure 4.10: Changes in concentration decay over time with changes in shear stress over the sand-gravel bed

that this effect may be muted by the bed characteristics (e.g. porosity). That said, experimental error prevents us from drawing a proportional mathematical relationship between u_* and α_1 for a given bed type.

The effect of the bed type can not only be seen in the general decay trends but in the concentration decay response to additional shear stress. The acrylic bed tests show dramatic changes in concentration decay with very small changes in shear stress (Figure 4.8). The porous bed tests show a much more muted response with comparatively larger changes in shear stress (Figures 4.9 and 4.10). This indicates that changes in shear velocity during instances of no bedload movement affect the deposition rate of clay to a porous bed to a lesser extent than the bed composition. Bed composition is the main contributor affecting the interaction of these particles.

4.3.6 Depositional Patterns

The location of deposited material generally followed two patterns, which coincided with the bed types being examined. Surface deposition dominated the non-porous acrylic bed tests while substrate deposition dominated the porous gravel and sand-gravel beds. Deposition on the acrylic bed formed patches of deposited clay which quickly became moving clay ripples, translating down the flume test section. The small, barchan-shaped dunes were surrounded and often fed by low speed streaks of saltating clay aggregates (Figure 4.11). Alternatively, the porous beds showed deposition near the surface and within the porous substrate with the visual majority of the deposition occurring closer to the surface (Figure 4.12). Deposition

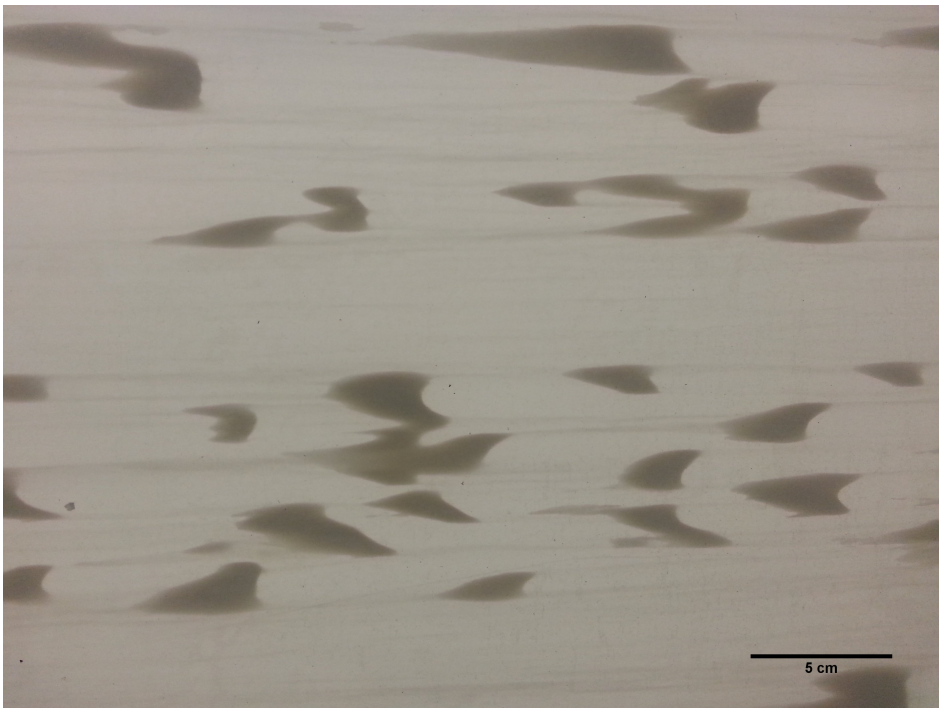

Figure 4.11: Dunes forming, moving, and combining amid low speed streaks during acrylic bed tests. Flow direction is from left to right. Approximate size of total figure is 33 cm by 25 cm.

on surface grains did occur but seemed to be limited to areas in the wake zone of surface grains. This implies that once particles were caught in these wake zones, they were able to settle through the interstitial voids of the substrate. The location of deposition, either at the surface or in the substrate, likely determines the amount of sediment available for entrainment during periods of increased bed shear stress.

4.4 The Entrainment Phase: Can Deposited Sediment Resuspend?

The entrainment phase was a period of increased bed shear stress above that of the deposition phase. This phase was included at the end of the deposition phase of each experimental run to test whether increased shear stress would cause deposited clay particles to entrain. It was

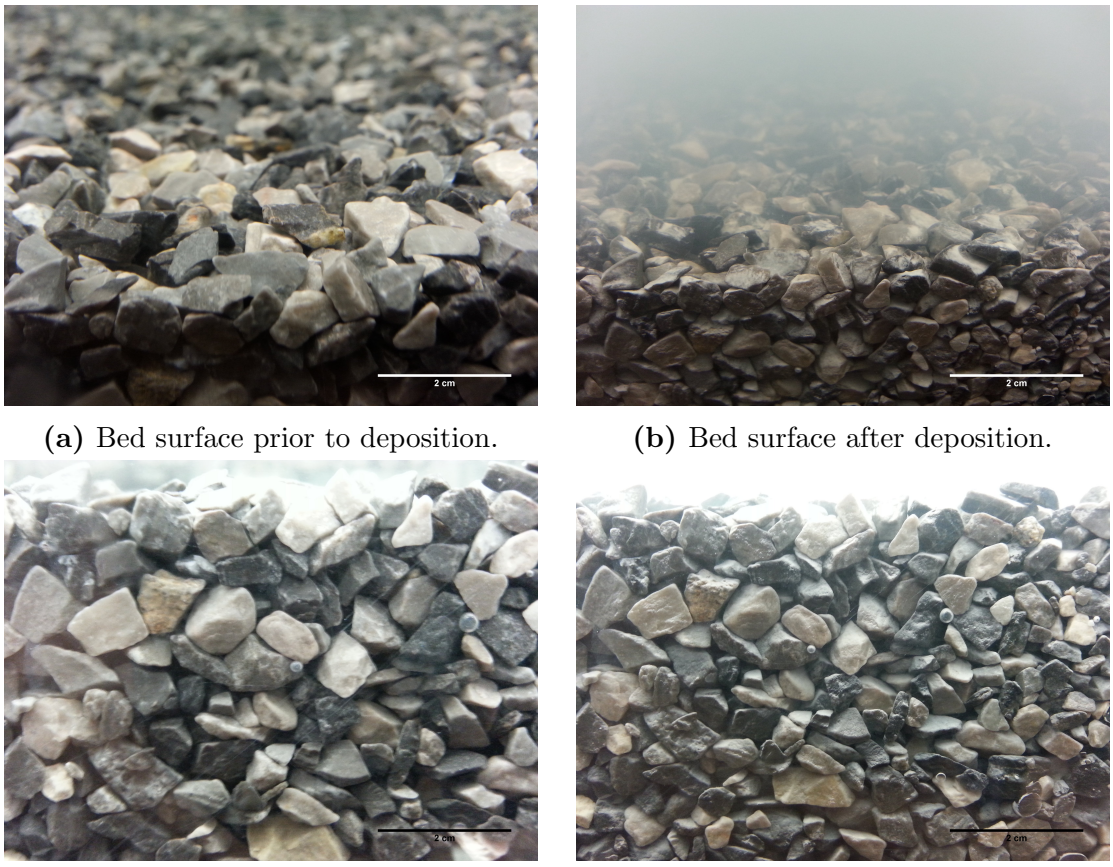

(a) Bed surface prior to deposition.

(b) Bed surface after deposition.

(c) Bed substrate prior to deposition.

(d) Bed substrate after deposition

Figure 4.12: Deposition within a porous gravel bed.

hypothesized that for porous beds, increased shear stress (below the threshold of bedload movement) would not cause entrainment of particles deposited below the bed surface.

The trends seen in the entrainment phase will be examined over two different time scales. A complete test was allowed to run for approximately twenty-four hours: ten hours for the deposition phase and fourteen hours for the entrainment phase. In the previous sections, only the first ten hours of the deposition phase were discussed. Large time scale trends include trends over the entirety of the fourteen hour entrainment phase, and may be directly compared to trends during the deposition phase. Large time scale observations allow us to say holistically whether increased shear (within the confines of no bedload movement) causes long term entrainment or continued deposition. Small time scales are those which surround the immediate time before and after the step increase in bed shear stress. This short time scale focuses on the immediate response of increased bed shear on the observed water column concentration.

4.4.1 Large Timescale Trends

An examination of the large time scale trends show a stark difference between the porous and non-porous beds (Figure 4.13). In the acrylic bed tests, increases in shear cause large increases in concentration - indicating that deposited sediment begins to entrain in the presence of increased bed shear stress. However, in the porous bed tests, the opposite long-term trend was observed. In the porous bed runs, periods of increased bed shear stress resulted in continual, near uninterrupted, decay of concentration with in the water column.

That is, continual uptake of mass by the bed occurred through the entire period of increased shear.

The results shown in light blue in Figure 4.13b are tests with very high bed shear stresses which did not have an entrainment phase. These tests are included to give the reader a sense of the shape of a continuous decay curve for reference during the entrainment period of the other tests. Since minimal or no bed deposition was observed in the highest shear tests over the acrylic bed (A:HS:HC) this was included as a reference (Figure 4.13a). Note, however, that this test does have a single entrainment phase observed at the start of the first vertical line. Also note that the trend after the last entrainment phase for all acrylic bed tests shows continuous decay of concentration. During these periods there were no bedforms observed in the flume channel. Furthermore, the low speed streaks which were present did not increase or decrease in size. This indicates that, at a certain point after total entrainment from the bed, decay in the rest of the flume system continued. This fits the theoretical model which accounts for continual system decay throughout the test. The theoretical framework is not yet sophisticated enough to account for the changes in entrainment and continued deposition at the same time as well as accounting for the source of entrainment. As such the raw data curves are shown in order to show the response of increased shear on interaction with the bed.

The results shown in Figure 4.13a not only highlight the response of bed entrainment, but also system entrainment. It is difficult, however, to determine the relative amount of entrained mass which originated from the channel bed or from increased shear in the

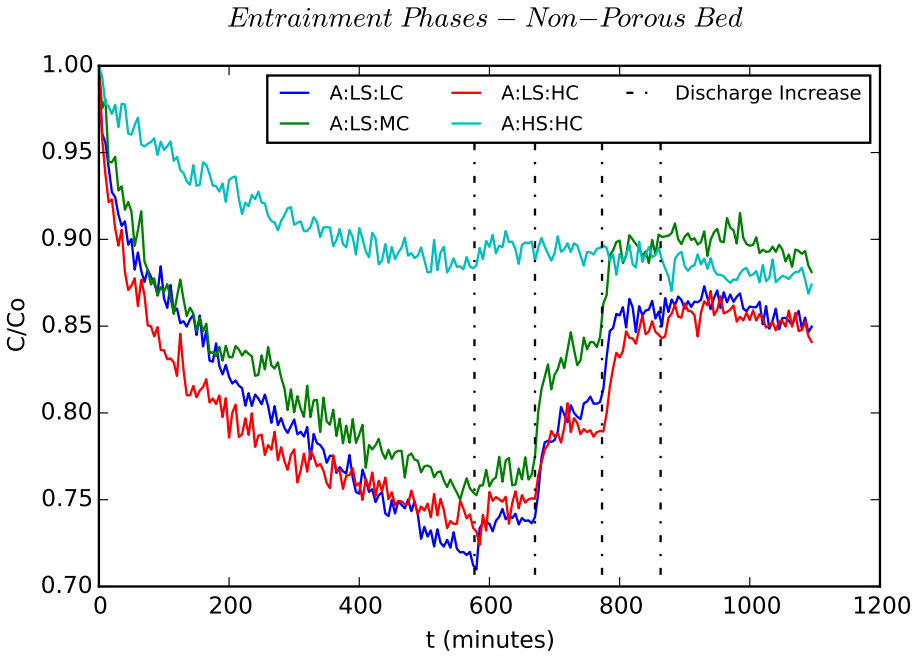

(a) Large scale trends during acrylic bed tests

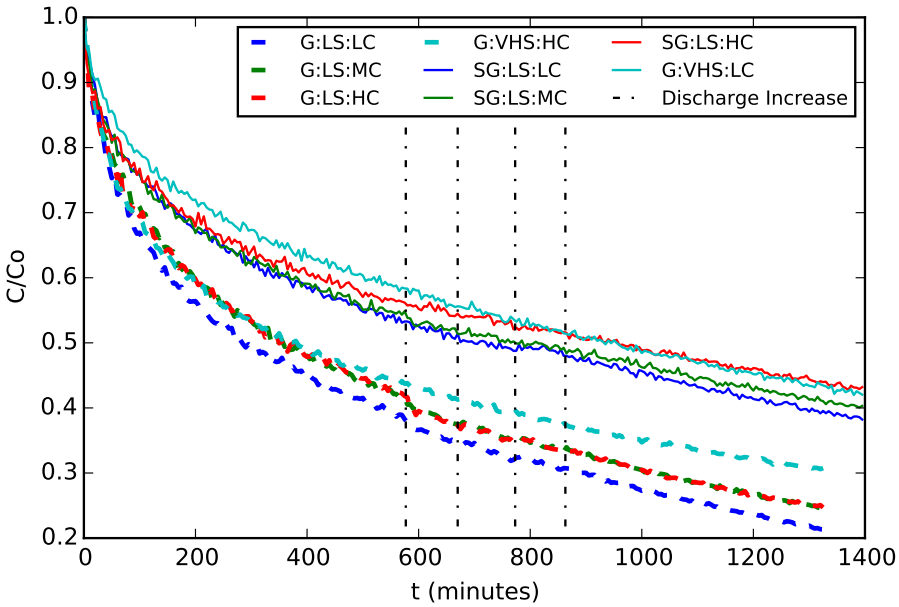

(b) Large scale trends during porous bed tests

Figure 4.13: Comparison of large timescale, entrainment phase trends between porous and non-porous bed types. The vertical bars indicate the times at which increases in shear stress occured.

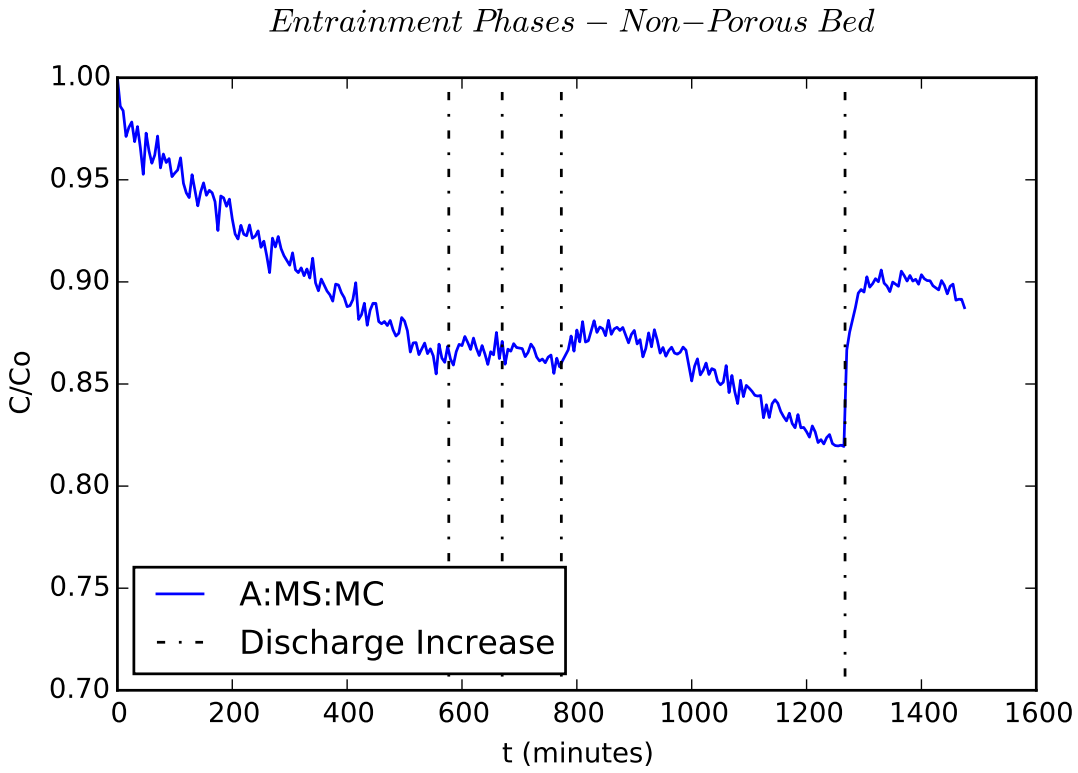

Figure 4.14: Large scale trends during A:MS:MC. During the last entrainment phase the flume was set to it's maximum discharge

pipes, headbox, or from deposition near the pump intake at the bottom of the tank. Visual inspection of the size of the bedforms was not detailed enough to estimate the change of mass present on the bed. That said, one acrylic bed test (A:MS:MC) did have an additional entrainment period where there was no bedform deposition, aside from stable low speed streaks. When discharge was increased during the final entrainment phase this caused a significant increase in observed concentration in the flume (Figure 4.14). This indicates that observed entrainment can come from the flume system. However, this does not help determine what portion of the observed entrained mass came from the bed or the system. A correlation can be drawn, however, between changes in observed bedform size and measured increases in concentration. The entrainment phase increases in concentration observed in Figure 4.13a correspond with reduction in the size and number of observed bedforms. These combined results indicate that a portion of this entrained mass came from the bed while another portion may have come from the system. Unfortunately, the relative quantities of that entrained mass cannot be determined with the data available.

4.4.2 Small Timescale Trends

The small time scale trends for the acrylic glass tests will not be examined in this section. These trends are very evident as shown in Figures 4.13a and 4.14. However, small time scale entrainment trends for the porous beds will be examined. These trends (Figure 4.15) show small responses in increased concentration with increases in bed shear stress. These are most noticeable at certain bed shear stresses. These trends differ from those observed in

the acrylic glass tests in that some increases in shear stresses cause greater deposition to the bed. These occur in the Gravel Tests during the shift from $u_* = 0.0191$ m/s to $u_* = 0.0251$ m/s (i.e. the beginning of the first entrainment phase). Subsequent increases in shear stress either cause a small increase in concentration or no observable increase in concentration followed by continual decay at a similar rate.

The observed small shifts in concentration can be seen as phase shifts where the concentration changes but the general shape of the decay curve does not change. Shifts in concentration to or from the bed are more evident in the gravel bed tests than in the sand-gravel bed tests. Similar to the acrylic glass tests, it is not possible to determine if an increase in mass in the water column is caused by entrainment from the bed, the system, or both. However, increased shear stress in the system pipes and headbox would most likely not cause a decrease in concentration as observed during the first entrainment phase in Figure 4.15a. This shift must have been a result of increased deposition to the bed during the short period of time just after discharge was increased.

In applying these results to the theoretical framework one can conclude that for smooth, non-porous beds increases in shear stress can cause entrainment of deposited wash load material. The results of entrainment over porous beds shows that without movement of the bed framework material, higher bed shear stress does not result in large entrainment of deposited material. It is impossible to say if entrainment observed in the porous bed tests came from the system or from the surface. Since the increases in observed concentration were so small we cannot conclude if any deposited clay entrained at all. Observations of

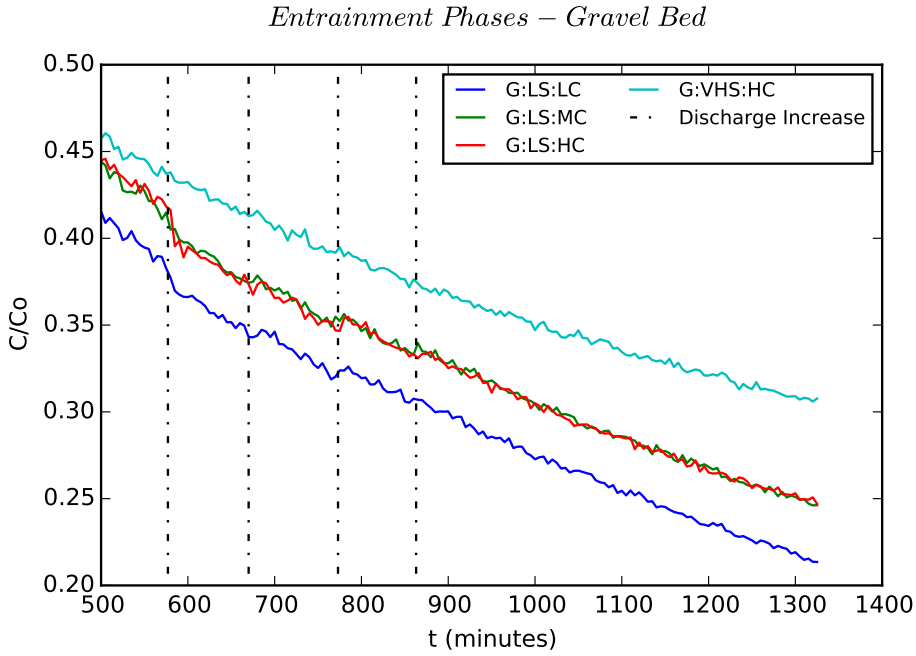

(a) Small scale trends during the gravel bed tests. Note: Test G:VHS:HV does not have any entrainment phases.

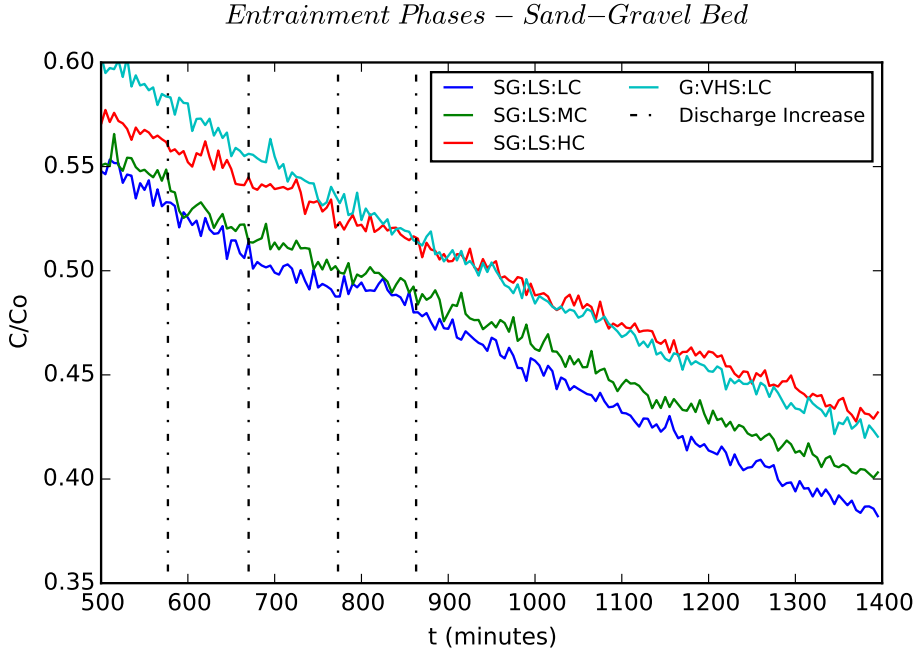

(b) Small scale trends during the sand-gravel bed tests

Figure 4.15: Comparison of small timescale, entrainment phase trends during porous bed tests. The vertical bars indicate the times at which increases in shear stress occured.

the substrate over the entrainment period did not show an observable decrease in deposited material. Because deposition continued over the entire entrainment phase for the porous beds the small time scale changes in concentration would not be observable in the quantity of deposited clay. Continued research in which the experimental apparatus is modified so there is no system deposition is required in order to better determine the entraining properties of increased shear stress on clay deposited in porous beds.

5 Discussion

5.1 Hypotheses

In answering the first experimental question it was hypothesized that the suspended sediment flux to the bed was a function of the bed type and bed shear stress, but not a function of initial concentration. The results from these tests, in line with others (Lau and Krishnappan, 1994; Mehta and Partheniades, 1975), show that the normalized decay rate of concentration in the water column is not a function of initial concentration given constant bed type and bed shear stress. That does not mean that a higher concentration will not deposit more mass to the bed. It simply means that the decay in concentration will be the same percentage over time. That is, if a certain bed shear stress causes 40% of the suspended sediment to deposit over some given time then that is the fraction of suspended sediment that will deposit in the given time regardless of the initial concentration in the stream. More importantly, the experiments showed that the mass decay rate is a function bed composition and bed shear stress. Of these two conditions, the bed characteristics are the driving factor which govern the deposition of suspended clay. Changes in shear stress have muted or enhanced abilities to change the decay rate for porous and non-porous beds, respectively.

In answering the second experimental question it was hypothesized that suspended

wash load would deposit within the substrate of porous beds. Test results indicate that deposition occurred within the gravel bed and the open framework gravel armor layer of the sand-gravel bed. Significant deposition past the sand layer of the sand-gravel bed was not observed, though it is possible that some clay made it into the sand layer. Calculation of the critical clogging factor using the Huston and Fox (2015) criteria suggests that the void space between the sand grains was too small to allow for static percolation of the clay aggregates. Deposition occurred near the surface of the porous beds but only in the wake zones of surface grains. All other deposition was within the substrate. Deposition also occurred on the acrylic bed and formed ripples which moved down the test channel.

In answering the third experimental question it was hypothesized that material deposited in porous beds will not be available for re-entrainment due to increases in bed shear stress as long as there is no bed load movement. That is, the material is lost to the bed until the surface layer is fully mobilized. The experimental results indicate that some entrainment occurs but the source of the entrainment (e.g., from the bed or the system) could not be determined. Despite some entrainment the overall interaction during periods of higher shear stress was continued mass flux to the bed. As long as the bed was stable deposition continued. Conversely, increased bed shear stress over the acrylic bed caused visible entrainment of deposited bed forms. It is therefore concluded that the entire deposition on the acrylic bed was available for entrainment while hiding effects caused only a minimal amount of deposition on the porous beds to be available for entrainment.

The results in this study beg the question, why do suspended clay particles deposit to

porous and non-porous beds despite the fact that the Rouse Number is so low? For instances where $P \ll 1$ one would expect that any material deposited to the bed would quickly re-entrain as the entraining properties of the flow completely dominate the settling velocity. It is suspected that the answer to this lies in the hiding effects associated with the viscous sublayer and in separated wake zones of surface grains.

5.2 Acrylic Bed Deposition

It can be shown that the acrylic bed tests were all run under hydraulically smooth conditions ($k_s^+ < 4$ where $k_s^+ = u_* k_s/\nu$). As such, the experiments over the acrylic bed all had a viscous sublayer whose depth can be approximated as,

$$\delta = \frac{11.6\nu}{u_*} \tag{5.1}$$

where δ is the thickness of the viscous sublayer, and ν is the kinematic viscosity. Following equation 5.1, viscous sublayer thickness for the acrylic bed tests ranged from 0.35 mm to 0.61mm. Given that the largest size particles in suspension at the beginning of the test were 0.0365 mm in diameter, it is reasonable to conclude that particles deposited on the bed fell within the viscous sublayer. This was evidenced by the presence of low speed streaks (Kline et al., 1967) throughout the flume channel (Figure 5.1).

Though deposition and bedload movement of clay within the low speed streaks accounts for some deposition, it does not account for the majority of deposition. That is because low speed streaks such as these did not deposit the mass required to drastically change the

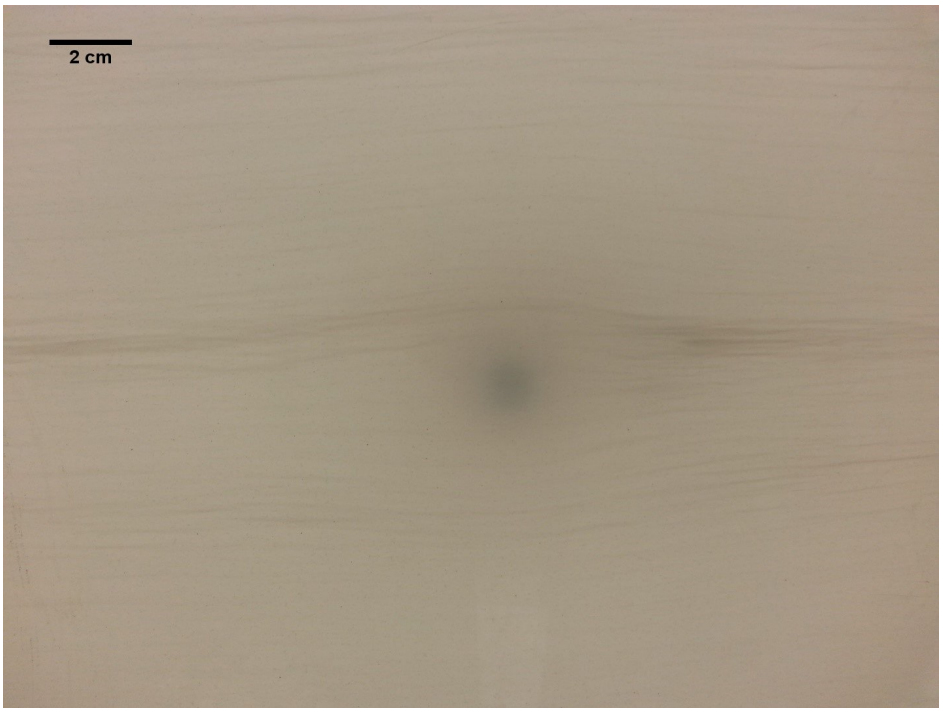

Figure 5.1: Visual of low speed streaks in the viscous sublayer. Flow is moving from left to right. Image view is from below the flume channel. Scale is approximate.

concentration in the water column over time. Though these streaks may have changed characteristics during the entraining period of the tests because of changes to the viscous sublayer during increases in bed shear stress, the main depositional period of the tests did not have this change. The mass required to change the concentration as read in the flume was observed in the formation of clay ripples on the bed.

During the initial acrylic bed tests, the flume channel would naturally form small bubbles which would adhere to the flume bottom at low shear stresses. These bubbles were not measured but can be said to exist within and likely protrude out of the viscous sublayer. In many cases these bubbles would remain adhered to the bottom of the flume through the depositional period of the test. These bubbles could be said to form small roughness

elements along the bed and would cause small regions of detached flow in their wake. This was evidenced in the deposition of clay particles in small bedforms in downstream bubble wakes (Figure 5.2). In some cases (Figure 5.2a) there is a pattern of low speed streaks feeding these bedforms which in turn feed subsequent low speed streaks downstream of the bubbles. This indicates that deposition of clay can occur in small wake zones over very smooth beds. Not only did this occur for isolated bubbles, but also for larger bubble fields which covered the width of the flume in some areas (Figure 5.2b).

The deposition process described above was enhanced by flocculation. Flocculation seldom occurs in recirculating flumes due to the highly turbulent nature of the recirculation system. This is partially confirmed in this study as imaged particles from the flow were, at least seemingly, resilient clay aggregates and not delicate clay flocs as found in estuaries and reservoirs. This may be a function of the recirculating pump, turbulence in the channel, and/or the process of sampling by pipette which may have caused any flocs present to break apart. Direct imaging of particles in the water column through the flume walls did not produce images clear enough to determine particle size or whether or not flocs were present. However, images of particles within the viscous sublayer taken through the flume clearly showed the presence of flocs. These flocs were in the near bed region and moved as bedload (Figure 5.3). Areas of near bed turbulence are said to break flocs apart and entrain them back to the water column which is what keeps small clay particles in suspension (Partheniades et al., 1968). The hydrodynamic and concentration conditions in the flume were in a range which preclude vertical floc size gradients in the water column (Winterwerp

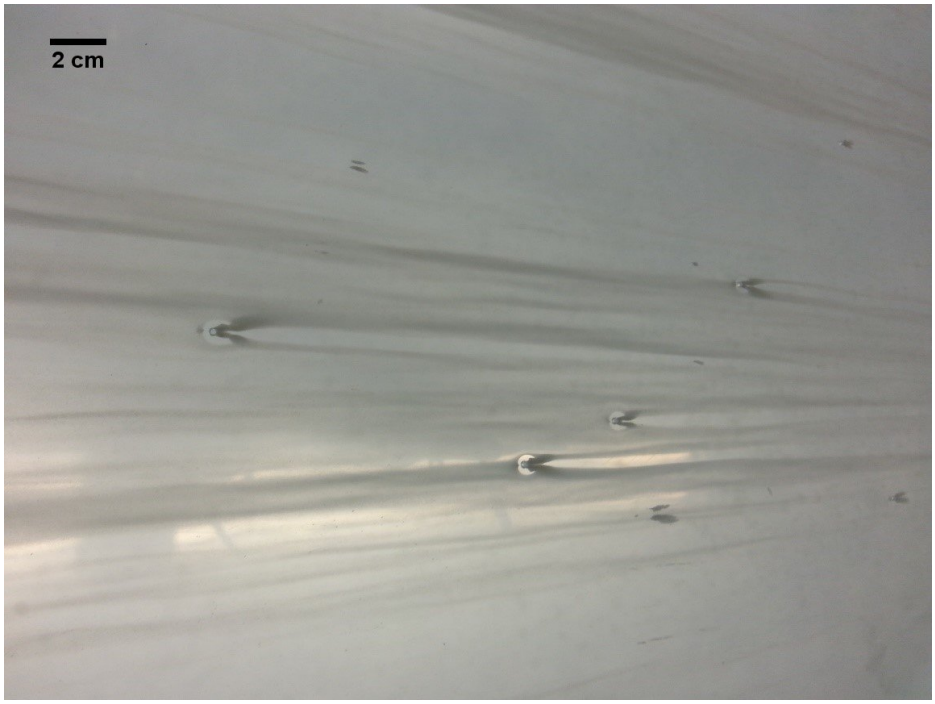

(a) Bubble deposition and low speed streaks. Flow is from left to right.

(b) Bubble deposition in a large field of bubbles. Flow is from right to left.

Figure 5.2: Wake zone deposition behind bubbles adhered to the acrylic bed surface. Image view is from below the flume channel. Scale is approximate.

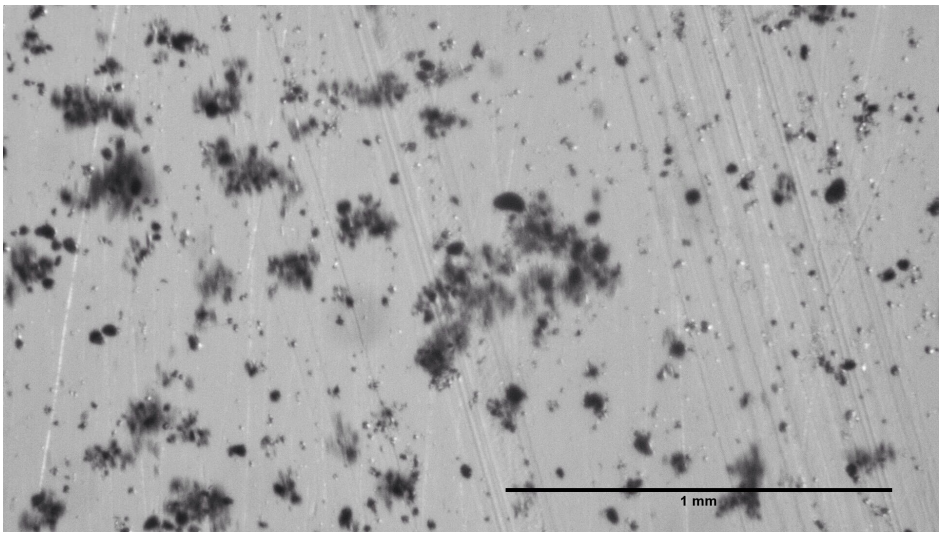

Figure 5.3: Floculation of clay within the within the viscous sublayer. Image view is from below the flume channel

and Van Kesteren, 2004). That is, flocculation and particle size are not functions of water column depth. Observed flocculation must then be occurring in the viscous sublayer, shielded from turbulent effects.

Bed deposition on the acrylic bed was not limited to low speed streaks and bubble wake zones. Across all but the highest shear stress tests clay ripples similar to those observed in Schieber et al. (2007) formed on the acrylic bed. These bedforms went through a series of stages in their development over time as they initially settled, developed in size, and began to move. These stages include: (1) initial formation, (2) bedform aggregation, and (3) bedform movement.

During initial formation, bedforms developed ubiquitously over the downstream and span wise lengths of the flume. These bedforms did not form in any discernible or repeatable pattern or shape. The deposition on the bed in many cases appeared in a cheetah spot

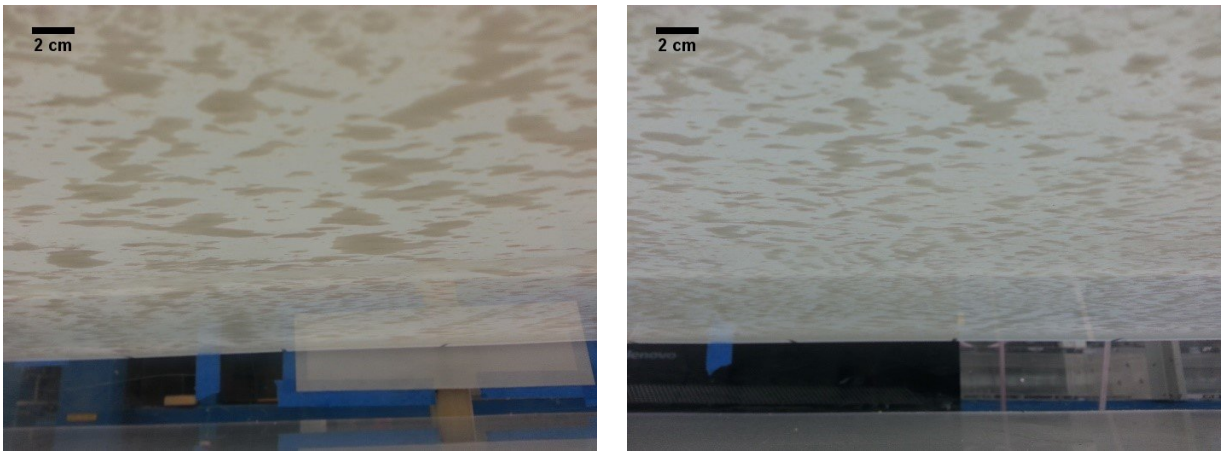

(a) **(b)**

Figure 5.4: Phase 1 deposition. Image view is from below the flume channel. Note the random deposition pattern evenly across the spanwise direction of the bed. Flow from right to left. Scale is approximate.

pattern. This pattern only emerged extensively in tests where shear velocity was at or below $u_* = 0.01$ m/s. For tests with greater shear stress this phase was not as extensive as shown in Figure 5.4 and bedforms quickly transitioned to bedform aggregation.

Bedform aggregation is a period marked by the movement and combining of initial bedforms into small barchan-shaped ripples. These ripples moved in a way similar to typical alluvial and aeolian ripples and dunes: entrainment of particles would occur on the stoss and deposit in the lee-side wake zone. These dunes were heart shaped and would move as bedload along the bottom of the flume. Aggregation of bedforms would occur until the bedforms had grown to a sufficient size that they were no longer in the vicinity of other bedforms with which they could combine (Figure 5.5).

Bedform movement is a period marked by the stability of bedform size and movement downstream without combining with other bedforms. Though these bedforms would not

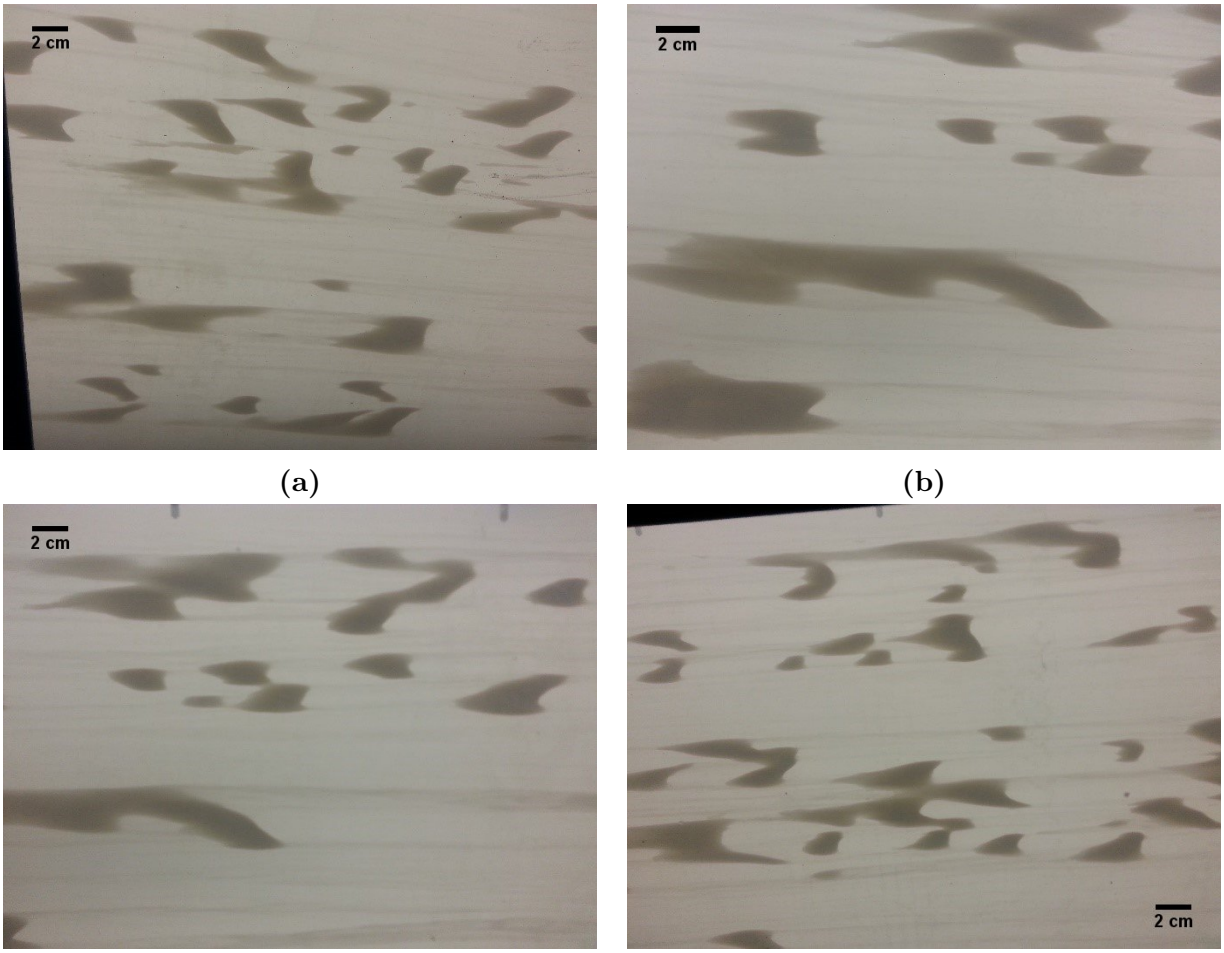

Figure 5.5: Phase 2 Deposition. Note the formation of heart-shaped bedforms and the subsequent aggradation of bedforms which are in close proximity to each other. Flow in all figures is from left to right. Scale is approximate.

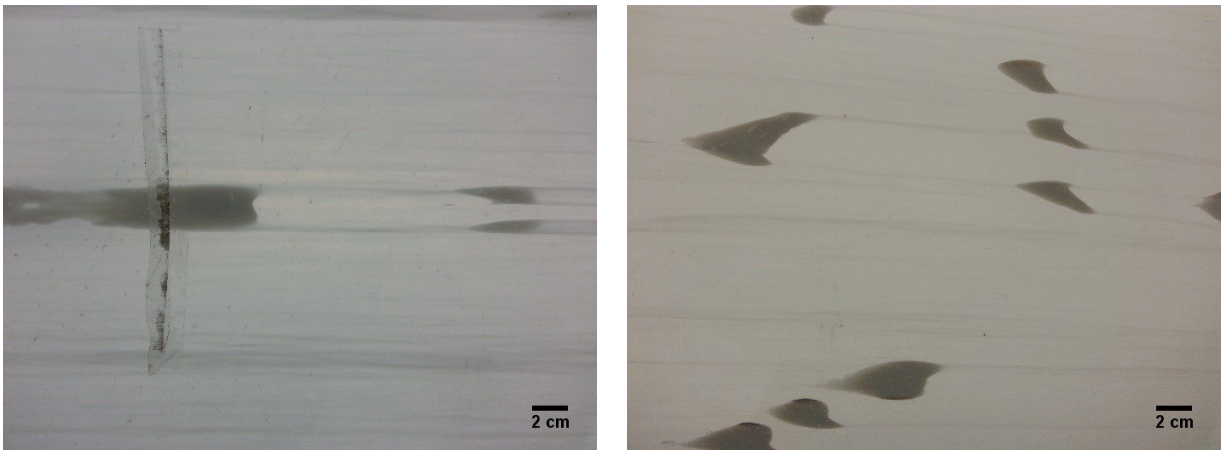

(a) **(b)**

Figure 5.6: Phase 3 deposition. Clay dunes feeding other dunes through low speed streaks. These trends existed on a larger scale but it was not possible to photograph them given their separation distance. Scale is approximate.

aggregate during this period they did supply each other with material through trailing edge sediment streams (Figure 5.6). That is, a clay ripple was fed from the upstream by a low speed streak or trailing edge sediment stream at the base of the stoss. Upon reaching the stoss, sediment would be dispersed around and over the bedform with some of the material being deposited in the wake zone. The remaining portion of the incoming sediment, along with some material sourced from the other parts of the bedform, would then leave from the outer lateral corners of the bedform wake. These streams of sediment would then feed other bedforms downstream. In moving like this the clay dunes alternated so that one did not form directly behind the other but was offset by the dune width (Figure 5.6).

5.2.1 Gravel Bed Deposition

The smooth and rough boundary tests differ in their bed roughness and bed porosity. Surface roughness of the gravel particles prevented the formation of a large-scale viscous sublayer

because the gravel roughness length scale ($z_0 = 0.25d_{50} = 1.05$ mm) was larger than the viscous sublayer depth. However, the surface gravel grains could be said to produce a large field of obstructions similar to the bubbles formed on the smooth bed. Unlike the acrylic bed test, the area below the gravel wake zones was a porous bed into which the depositing clay particles could settle. These conditions prevented the formation of large dune-like bedforms on the rough boundary. However, deposition in these beds was observed in the wake zones of other grains (Figure 5.7). Sediment captured within these wake zones was then able to settle through the interstitial voids of the bed until deposition occurred on a given substrate grain.

Deposition of clay within the substrate was stratified in the presence of relatively low bed shear. More deposition occurred near the surface and progressively less deposition deeper in the substrate (Figure 5.7). Figures 5.7a and 5.7b show the bed surface and substrate, respectively, prior to deposition beginning. As deposition increases the deposition near the surface (Figures 5.7c, 5.7e) is visibly greater than that deep within the substrate (Figures 5.7d, 5.7f). It is theorized that many of these particles did not settle further into the bed because the likelihood of not depositing decreases with increasing depth into the substrate. There is no completely unimpeded path through the interstitial voids of the gravel. The further a given clay particle settles the more opportunity it has to deposit and the less likely it is to reach deeper areas of the substrate. Thus more particles settle near the surface and fewer settle deeper in the bed.

The time scale of deposition from the water column to the deepest parts of the sub-

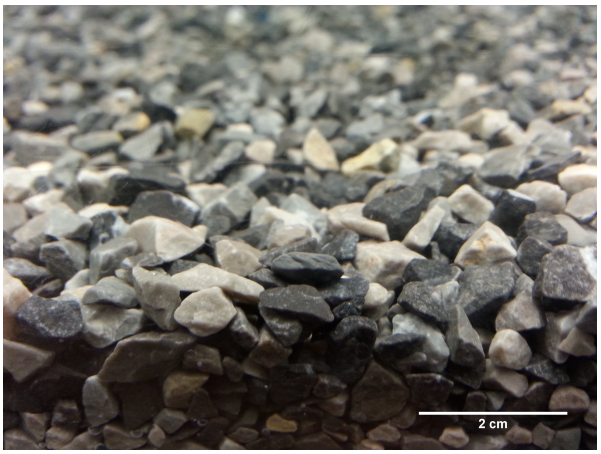

(a) Gravel surface prior to test

(b) Gravel substrate prior to test.

(c) Gravel surface at the end of the deposition period.

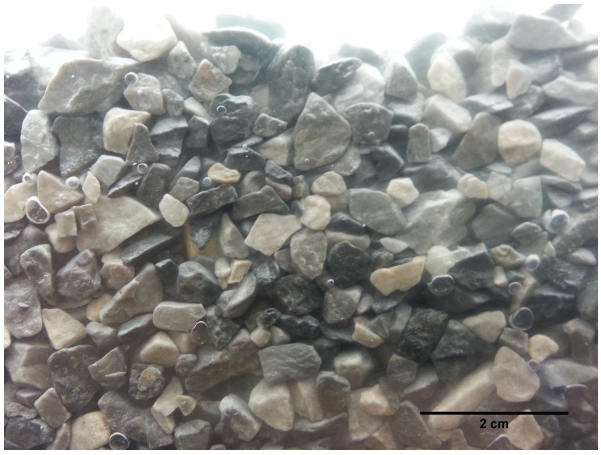

(d) Gravel substrate at the end of the deposition period.

(e) Gravel surface at the end of the entrainment period.

(f) Gravel substrate at the end of the entrainment period.

Figure 5.7: Depositional pattern of clay wash load in the gravel bed substrate. Note that surface deposition is in the wake zone of other surface elements and that deposition in the substrate is stratified with a higher proportion of clay deposited closer to the surface. Flow is from left to right. Pictures are taken from Test G:LS:HC. Scale is approximate.

strate could not be determined by the experimental setup. Particles may have settled on grains protected by wake zones and later dislodged to settle deeper into the substrate. This would result in a large deposition timescale for particle settling. Likewise, the vertical clay deposition pattern could be simply a result of bed filtering with only a small amount of clay mass able to reach the deeper substrate depths. This would result in a reduced depositional timescale for each individual particle.

This depositional pattern does not change when shear stress is increased during the entrainment period. It is difficult to determine the change because the mass deposited in the bed was greater in the depositional period than in the entrainment period. Furthermore, given there could be system entrainment additional clay could have become available to deposit in the bed after the entrainment period started. Patterns in near surface deposition were dissimilar for deposition phases of different shear stresses (Figure 5.8). The two presented graphics show gravel surfaces before and after the deposition phase of tests G:LS:MC and G:HS:MC. Note the higher visual deposition for the lower shear stress test. This indicates that shear stress plays a factor in deposition location. Cohesion likely plays a factor in deposited clay's resistance to entrainment from near surface areas (Figure 5.7) and the reduction in deposition while under similar hydraulic conditions (Figure 5.8). The deposited clay may be resistant to entrainment due to cohesion whereas it is less likely to deposit on the surface in the first place under the same hydraulic conditions.

In order to determine the settling process a series of video recordings were taken of the surface roughness layer, magnified by a 15 power magnifying lens. Observations showed that

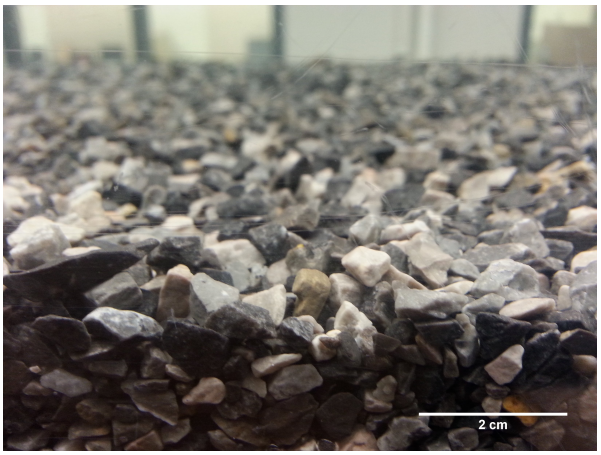

(a) Test G:LS:MC prior to deposition phase.

(b) Gravel test 4 after deposition phase.

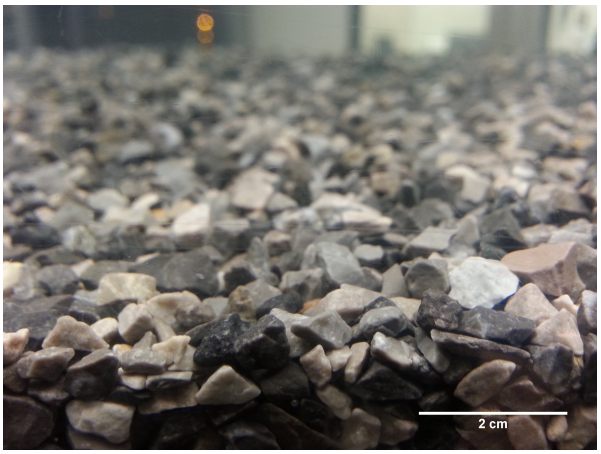

(c) Test G:HS:MC prior to deposition phase.

(d) Test G:HS:MC after deposition phase.

Figure 5.8: Surface deposition during the deposition phase of two separate shear stresses. Surface deposition patterns between the two tests are minimal. Scale is approximate.

small clay particles would settle unimpeded through the interstitial voids of the substrate. These particles were large enough that they could be viewed with a relatively low power magnifying lens. This means that the settling particles were either large aggregates which had settled out early in the test or flocculated particles which were heavy enough to settle into the substrate. The low shear stress within the void space provides an area where flocculation could occur which would lend credence to the idea that flocculation in the pore space causes settling. Lighting limitations prevented the sizing of settling particles within the substrate with the Point Grey camera and the suspended sediment characteristics could not be confirmed.

5.2.2 Sand-Gravel Bed Deposition

As discussed earlier the sand-gravel beds formed an armor layer of gravel particles which rested above the sand-gravel mixture. Deposition within the sand-gravel bed was similar to that of the gravel bed in that particles were able to settle through the interstitial voids of gravel particles at the surface. The depth of deposition within the sand-gravel beds was limited by the presence of the sand layer. At this location the void space of the sand was small enough that it prevented further settling (Figure 5.9).

Note that the amount of sand in the bed was not sufficient to classify it as bimodal but still limited the depth of settling wash load. This caused the entirety of the deposited clay to settle within the armor layer and thus closer to the effects of bed shear stress. Despite this, increases in shear stress did not cause substantive entrainment from the bed. In fact,

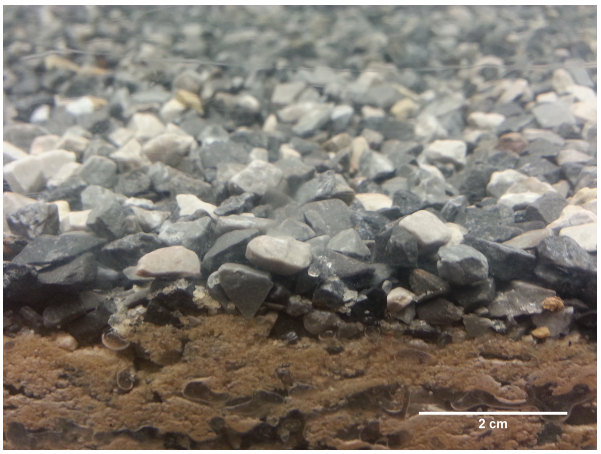

(a) Test SG:LS:HC bed surface prior to deposition phase.

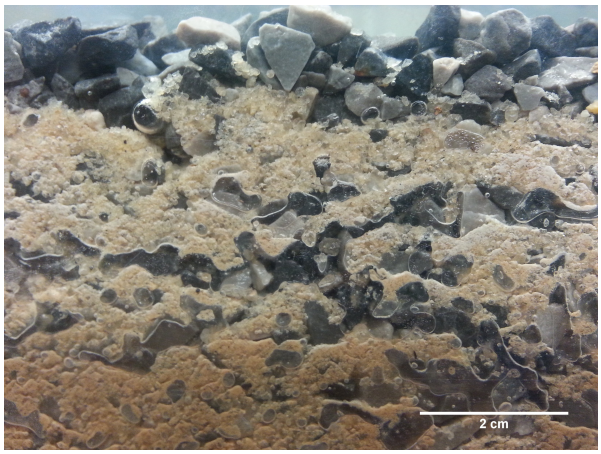

(b) Test SG:LS:HC bed substrate prior to deposition phase.

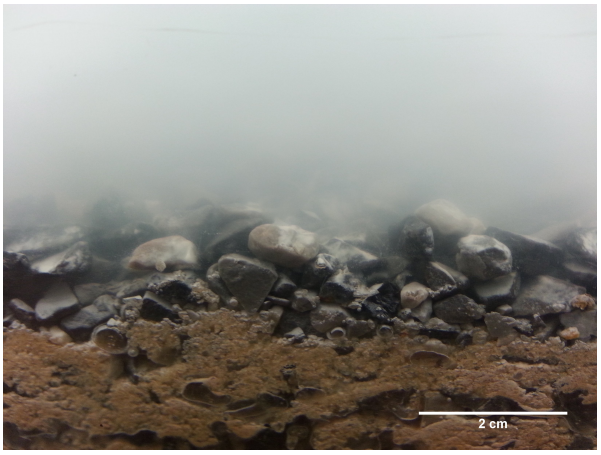

(c) Test SG:LS:HC bed surface after the deposition phase.

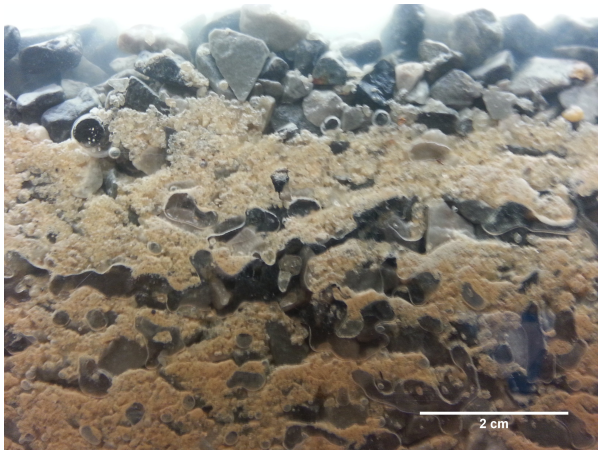

(d) Test SG:LS:HC bed substrate after the deposition phase.

(e) Test SG:LS:HC bed surface after the entrainment phase.

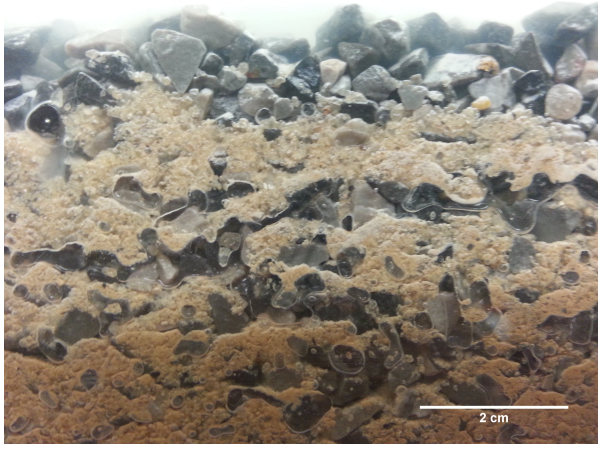

(f) Test SG:LS:HC bed substrate after the entrainment phase.

Figure 5.9: Deposition patterns at the surface and in the substrate of the sand-gravel bed. Scale is approximate.

the trend of continual long term deposition and retention of surface deposition during the entrainment phase as seen in the gravel bed is the same in the sand-gravel bed. Near surface deposition also changed between tests with higher depositional phase shear stresses (Figure 5.10). This trend was also seen in the gravel bed tests. That said, the small depth of the armor layer may indicate that all deposition is in the near surface region. Deposition in the sand-gravel bed tests was smaller than that of the gravel bed tests so this difference may simply be a lack of overall deposition in the armor layer due to the reduced area of potential settling.

These results have three major implications. First, wash load can deposit into gravel beds with even small armor layers as the effects of shear stress are limited below the roughness elements. Second, clogging of interstitial voids can occur below the armor layer for gravel substrates which contain relatively small amounts of sand. Third, if bedload movement causes deposited wash load to entrain then only minimal bedload movement may be required to entrain large portions of deposited wash load in bimodal gravel beds.

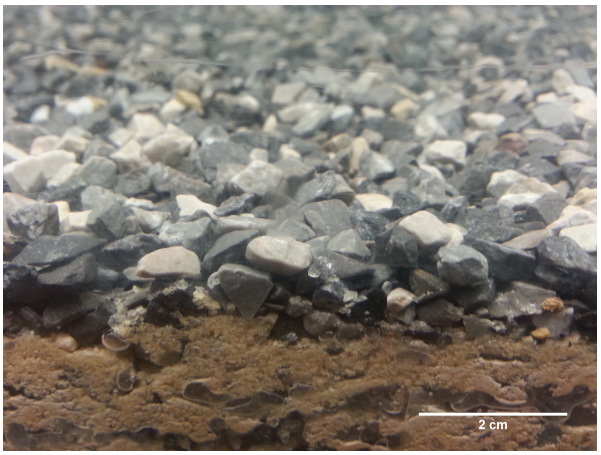

(a) Test SG:LS:HC bed surface prior to deposition phase.

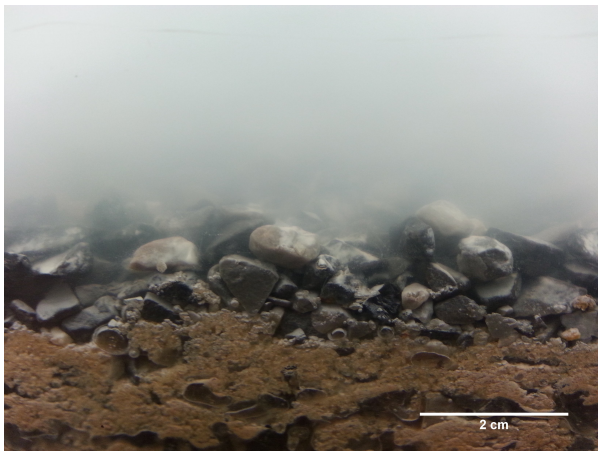

(b) Test SG:LS:HC bed surface after the deposition phase.

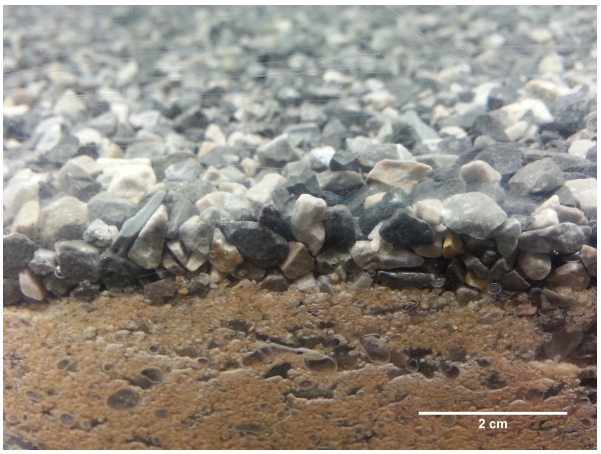

(c) Test SG:HS:HC bed surface before the deposition phase.

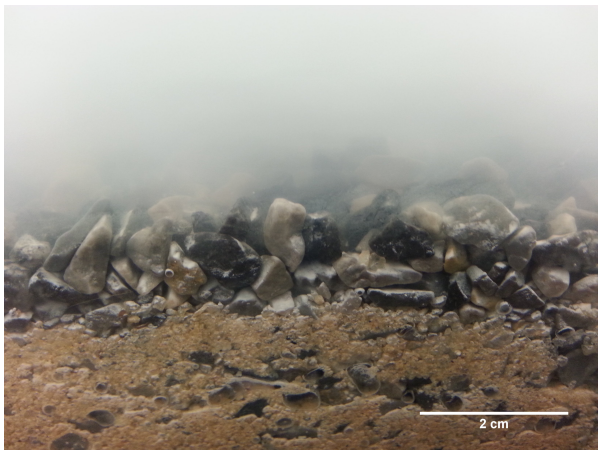

(d) Test SG:HS:HC bed surface after the deposition phase.

Figure 5.10: Deposition patterns near the surface the sand-gravel bed during depositional phases of low and high shear stress, respectively. Scale is approximate.

6 Conclusions

A series of wash load deposition and entrainment experiments were conducted in the Kelso Baker Environmental Hydraulics Laboratory at Virginia Tech. These tests involved characterizing the deposition of kaolinite clay from the water column to a series of porous and nonporous beds meant to simulate unimodal and bimodal gravel beds. This involved developing and testing a mass conservation model which describes mass flux to the bed in a recirculating flume where settling must be accounted for in the test channel and flume system.

The evidence from this study indicates several facts about wash load interaction with gravel beds. These include that under hydraulic conditions where the bed load does not move, there is deposition of clay wash load to various types of porous and non-porous beds. Deposition formed moving, mud bedforms over the non-porous acrylic glass bed. Deposition in the porous beds occurred primarily in the substrate. Interaction of suspended particles with the viscous sub layer and wake zones is key in understanding the deposition of wash load over these beds. Characterizing this interaction will give engineers a heightened understanding of the mechanics involved in moving very fine particles from a highly turbulent flow to settling in pore water. The decay of this deposition is most highly controlled by the characteristics of the bed material and to a lesser extent the bed shear stress. Results in

this study also confirmed observations in the literature where the normalized concentration decay is not a function of the initial concentration.

It has been shown that entrainment can occur from non-porous beds. However, the experiments were inconclusive in showing that entrainment can occur from porous beds. The inability to determine this was due to system decay and entrainment in the flume system outside the channel bed. Nevertheless, one can say that less material is available for re-entrainment when clay particle settle within the void space of a gravel or gravel-sand bed. This is significant as it implies that wash load lost to the bed is essentially sequestered until the surface layer begins to move as bed load. Further research is required in order to experimentally confirm this hypothesis.

It was observed that spatial deposition within porous beds is dependent upon the bed composition. The Huston and Fox (2015) threshold was the best predictor of static percolation versus clogging layer development by settling sediment. For the gravel bed this involved static percolation throughout the substrate. For the sand-gravel bed this involved static percolation through the armor layer and accumulation of deposited clay at the surface of the sand-gravel substrate. It is hypothesized that the thickness and composition of the armor layer would have a direct relationship on the decay rate of wash load to bimodal gravel beds.

Bibliography

Antonia, R. and Luxton, R. (1971). The response of a turbulent boundary layer to a step change in surface roughness. part 1. smooth to rough. *Journal of Fluid Mechanics*, 48(4):721–761.

Barzilai, R., Larrone, B., and Reid, I. (2013). Effect of changes in fine grained matrix on bed load sediment transport in a gravel bed river. *Earth Surface Processes and Landforms*, 38:441–448.

Berkman, H. E. and Rabeni, C. (1987). Effect of siltation of stream fish communities. *Environmental Biology of Fishes*, 18(4):441–448.

Beschta, R. L. and Jackson, W. (1979). The intrusion of fine sediments into a stable gravel bed. *Fish Res. Board Canada*, 36:204–210.

Carling, P. A. and Reader, N. A. (1982). Structure, composition, and bulk properties of upland stream gravels. *Earth Surface Processes and Landforms*, 7(4):349–365.

Church, M. and Hassan, M. (1998). Stabalizing self-organized structures in gravel-bed stream channels: field and experimental observations. *Water Resources Research*, 34(11):3169–3179.

Colby, B. (1957). Relationship of unmeasured sediment discharge to mean velocity. *Transactions American Geophysical Union*, 38(5):708–717.

Dermisis, D. and Papanicolaou, A. T. (2014). The effects of protruding rock boulders in regulating sediment intrusion within the hyporheic zone of mountain streams. *Journal of Mountain Science*, 11(6):1466–1477.

Einstein, H. (1968). Deposition of suspended particles in a gravel bed. *J. Hydraul. Eng*, 94(5):1197–1205.

Einstein, H., Anderson, A. G., and Johnson, J. W. (1940). A distinction between bed-load and suspended load in natural streams. *Eos, Transactions American Geophysical Union*, 21(2):628–633.

Elliot, A. and Brooks, N. (1997). Transfer of nonsorbing solutes to a streambed with bed forms: Laboratory experiments. *Water Resour. Res*, 33(1):137–151.

Garcia, M. H. (2008). Sediment transport and morphodynamics. *Sedimentation engineering: Processes, measurements, modeling, and practice*, (110).

Garcia-Aragon, J., Droppo, I. G., Krishnappan, B., Trapp, B., and Jaskot, C. (2011). Experimental assessment of Athabasca River cohesive sediment deposition dynamics. *Water Quality Research Journal of Canada*, 46(1):87–96.

Gibson, S., Abraham, D., Heath, R., and Schoellhamer, D. (2009). Vertical gradational variability of fines deposited in a gravel framework. *Sedimentology*, 56(3):661–676.

Haralampides, K., McCorquodale, J. A., and Krishnappan, B. (2003). Deposition properties of fine sediment. *Journal of Hydraulic Engineering*, 129(3):230–234.

Hudson-Edwards, K. (2003). Sources, mineralogy, chemistry and fate of heavy metal-bearing particles in mining-affected river systems. *Mineralogical magazine*, 67(2):205–218.

Huston, D. L. and Fox, J. F. (2015). Clogging of fine sediment within gravel substrates: Dimensional analysis and macroanalysis of experiments in hydraulic flumes. *Journal of Hydraulic Engineering*, 141(8):04015015.

Kline, S., Reynolds, W., Schraub, F., and Runstadler, P. (1967). The structure of turbulent boundary layers. *Journal of Fluid Mechanics*, 30(04):741–773.

Krishnappan, B. and Engel, P. (2006). Entrapment of fines in coarse sediment beds. In *River flow*, pages 817–824.

Krishnappan, B. G. (2000). Modelling cohesive sediment transport in rivers. *IAHS Publication(International Association of Hydrological Sciences)*, (263):269–276.

Krishnappan, B. G. (2007). Recent advances in basic and applied research in cohesive sediment transport in aquatic systems. *Canadian Journal of Civil Engineering*, 34(6):731–743.

Krone, R. B. (1962). Flume studies of the transport of sediment in estuarial shoaling processes. *Final Report Hydraulic Engineering Laboratory and Sanitary Engineering Research Laboratory, University of California, Berkeley, USA*.

Krone, R. B. (1993). Sedimentation revisited. *Nearshore and estuarine cohesive sediment transport*, pages 108–125.

Lambert, C. and Walling, D. (1988). Measurement of channel storage of suspended sediment in a gravel-bed river. *Catena*, 15(1):65–80.

Lau, Y. and Krishnappan, B. (1992). Size distribution and settling velocity of cohesive sediments during settling. *Journal of hydraulic Research*, 30(5):673–684.

Lau, Y. and Krishnappan, B. (1994). Does reentrainment occur during cohesive sediment settling? *Journal of Hydraulic Engineering*, 120(2):236–244.

Leopold, L. (1992). Sediment size that determines channel morphology. *Dynamics of gravel-bed rivers*, pages 297–311.

Lisle, T. E. (1989). Sediment transport and resulting deposition in spawning gravels, north coastal california. *Water resources research*, 25(6):1303–1319.

Mehta, A. J. and Partheniades, E. (1975). An investigation of the depositional properties of flocculated fine sediments. *Journal of Hydraulic Research*, 13(4):361–381.

Merrington, G. and Alloway, B. (1994). The transfer and fate of Cd, Cu, Pb and Zn from two historic metalliferous mine sites in the UK. *Applied Geochemistry*, 9(6):677–687.

Middleton, G. V. and Southard, J. B. (1984). *Mechanics of Sediment Movement*. SEPM.

Nagaoka, H. and Ohgaki, S. (1990). Mass transfer mechanism in a porous riverbed. *Water Res*, 24(4):417–425.

Packman, A. I. and Brooks, N. H. (1995). Colloidal particle exchange between stream and stream bed in a laboratory flume. *Marine and freshwater research*, 46(1):233–236.

Packman, A. I., Brooks, N. H., and Morgan, J. J. (1997). Experimental techniques for laboratory investigation of clay colloid transport and filtration in a stream with a sand bed. In *The Interactions Between Sediments and Water*, pages 113–122. Springer.

Packman, A. I., Brooks, N. H., and Morgan, J. J. (2000a). Kaolinite exchange between a stream and streambed: Laboratory experiments and validation of a colloid transport model. *Water Resources Research*, 36(8):2363–2372.

Packman, A. I., Brooks, N. H., and Morgan, J. J. (2000b). A physicochemical model for colloid exchange between a stream and a sand streambed with bed forms. *Water Resources Research*, 36(8):2351–2361.

Packman, A. I., Salehin, M., and Zaramella, M. (2004). Hyporheic exchange with gravel beds: basic hydrodynamic interactions and bedform-induced advective flows. *Journal of Hydraulic Engineering*, 130(7):647–656.

Parker, G. (2008). Transport of gravel and sediment mixtures. *Sedimentation engineering: Processes, measurements, modeling, and practice*, 110:165–252.

Parker, G. and Andrews, E. (1985). Sorting of bed load sediment by flow in meander bends. *Water Resources Research*, 21(9):1361–1373.

Partheniades, E. (1965). Erosion and deposition of cohesive soils. *Journal of the Hydraulics Division*, 91(1):105–139.

Partheniades, E., Cross, R. H., and Ayora, A. (1968). Further results on the deposition of cohesive sediments. In *Proceedings, 11th Conference on Coastal Engineering, London, England*, volume 2, pages 723–742.

Peng, J.-f., Song, Y.-h., Yuan, P., Cui, X.-y., and Qiu, G.-l. (2009). The remediation of heavy metals contaminated sediment. *Journal of hazardous materials*, 161(2):633–640.

Pizzuto, J. (2014). Long-term storage and transport length scale of fine sediment: Analysis of a mercury release into a river. *Geophysical Research Letters*, 41(16):5875–5882.

Platts, W. S. and Megahan, W. F. (1975). Time trends in riverbed sediment composition in salmon and steelhead spawning areas: South Fork Salmon River, Idaho. In *Trans. North Am. Wildl. Nat. Resour. Conf.*, number 40, pages 229–239.

Salomons, W. and Stigliani, W. (2012). *Biogeodynamics of pollutants in soils and sediments: risk assessment of delayed and non-linear responses*. Springer Science & Business Media.

Sanford, L. P. and Halka, J. P. (1993). Assessing the paradigm of mutually exclusive erosion and deposition of mud, with examples from upper Chesapeake Bay. *Marine Geology*, 114(1):37–57.

Schieber, J., Southard, J., and Thaisen, K. (2007). Accretion of mudstone bbeds from migrating floccule ripples. *Science*, 318:1760–1763.

Shaw, J. and Kellerhals, R. (1982). *The composition of recent alluvial gravels in Alberta river beds*. Alberta Research Council.

Shen, H. (1971). Wash load and bed load. *River mechanics*, 1:11–1.

Skalak, K. and Pizzuto, J. (2010). The distribution and residence time of suspended sediment stored within the channel margins of a gravel-bed bedrock river. *Earth Surface Processes and Landforms*, 35(4):435–446.

Smith, G., Nicholas, A., and Ferguson, R. (1997). Measuring and defining bimodal sediments: problems and implications. *Water Resources Research*, 33(5):1179–1185.

SonTek (2001). Acoustic doppler velocimeter (ADV) principles of operation. Sontek technical notes, Son Tek.

Tait, S., Willetts, B., and Maizels, J. (1992). *Laboratory observations of bed armouring and changes in bedload composition*. Wiley, New York.

Trefry, J. H. and Presley, B. J. (1976). Heavy metals in sediments from San Antonio Bay and the northwest Gulf of Mexico. *Environmental Geology*, 1(5):283–294.

Westrich, B. and Förstner, U. (2007). *Sediment dynamics and pollutant mobility in rivers: an interdisciplinary approach*. Springer Science & Business Media.

Winterwerp, J. C. and Van Kesteren, W. G. (2004). *Introduction to the physics of cohesive sediment dynamics in the marine environment*, volume 56. Elsevier.

Wood, P. J. and Armitage, P. D. (1997). Biological effects of fine sediment in the lotic environment. *Environmental management*, 21(2):203–217.